ANALYSIS OF AN EARTHQUAKE SWARM ASSOCIATED WITH THE CHRISTMAS, 1965 ERUPTION OF KILAUEA VOLCANO, HAWAII

A THESIS SUBMITTED TO THE GRADUATE DIVISION OF THE UNIVERSITY OF HAWAII
IN PARTIAL FULFILLMENT OF THE REQUIREMENTS FOR THE DEGREE OF

MASTER OF SCIENCE

IN GEOLOGY AND GEOPHYSICS

APRIL 1981

BY

RICHARD FRED BOSHER

Thesis Committee:

Frederick K. Duennebier, Chairman

David Epp

Michael O. Garcia

Mike G.

We certify that we have read this thesis and that in our opinion it is satisfactory in scope and quality as a thesis for the degree of Master of Science in Geology and Geophysics.

THESIS COMMITTEE

____

____

____

Mike,
Thanks for everything;
I really appreciate it.
Rob

ACKNOWLEDGMENTS

A most sincere and special thank you to Fred Duennebier, whose advice, optimism, and encouragement made this work possible. I am especially grateful to Dave Epp, Michael Garcia, Michael Ryan, Tom Brocher,and Ed Berg of the Hawaii Institute of Geophysics, and Fred Klein and Bob Koyanagi of the Hawaiian Volcano Observatory, United States Geological Survey, for their critical review and helpful suggestions in regards to this thesis. Many of the computer programs used in this study were modified with the assistance of John B. Sinton and Vindell Hsu.

The Hawaiian Volcano Observatory, United States Geological Survey, kindly provided the data for this study, and made their facilities available to the author while on the Big Island. A big mahalo to the HVO staff for their assistance and friendship.

Funds for this project were made possible through a grant from the National Science Foundation; Grant no: OCE76-82056A2, whose support is appreciated.

Last, and most importantly, to all my friends and my family, a hearty thank you for being there.

ABSTRACT

Locations, depths, magnitudes, and b-values have been determined for 419 earthquakes, which occurred during the time period December 24-30, 1965, in the Koae fault zone on Kilauea Volcano, Hawaii. This fault zone separates the south flank from the summit caldera of Kilauea. Extensive cracking in the Koae, and a minor east rift eruption accompanied the swarm. Statistical analysis and first motion studies were performed on selected earthquakes. A large percentage of earthquakes lie within the N70E trending Koae fault system. Focal depths range from 0 to 9 kilometers with an aseismic zone between 4 and 7 kilometers in the eastern Koae. An intrusive magma body, probably emplaced shortly after the swarm commenced, is inferred by this aseismic zone. Fault plane solutions and hypocentral distribution indicate extension along a zone of weakness in the central and western Koae, between 4 and 7 km depth, dipping approximately 30 degrees to the southeast. Seaward displacement of the south flank, away from the stable northern flank of Kilauea, can occur along this zone.

TABLE OF CONTENTS

LIST OF TABLES

LIST OF ILLUSTRATIONS

INTRODUCTION

This thesis reports on an earthquake swarm that occurred between December 24, and December 30, 1965, at Kilauea Volcano, Hawaii, and relates simultaneous geophysical events to geological processes of an active volcano. Extensive faulting and cracking in the Koae fault zone, a structural feature of the volcano, and a small eruption on the east rift zone of Kilauea accompanied the earthquake swarm (Fiske and Koyanagi, 1968). A seismic network maintained by the Hawaiian Volcano Observatory (HVO), United States Geological Survey, was in operation during the earthquake activity. From the available paper records, hypocentral locations, magnitudes, fault plane solutions, and location statistics have been determined for 419 earthquakes, which occurred from 13:00, December 25, to 08:00, December, 30, 1965. The initial earthquake activity commenced at 19:30, December 24. Due to large amplitude harmonic tremor (related to magma movement) and the high frequency of earthquakes, it was not possible to pick earthquakes which occurred from late December 24 to early December 25. The earthquakes analysed in this study had not been examined previously due to the high activity levels and shortage of manpower at HVO. The main thrust of this study is to reduce, analyse, and interpret the late December, 1965, seismicity. A large percentage of the located earthquakes lie within the Koae fault zone, or directly to the south. The known history of earthquake and eruption occurrence in the Koae is scant compared to the active summit and east rift zone of Kilauea (Duffield, 1975). The study of the unprecedented high levels of seismicity that occurred in the Koae during late December, 1965, provides a means for a better understanding of tectonic processes active in the Koae fault zone.

GEOLOGY AND TECTONICS

Kilauea Volcano is an active, basaltic, hotspot, shield volcano that forms the southeastern portion of the island of Hawaii (Fig. 1). Principal structural features of the volcano include; the summit caldera, the east rift zone, the southwest rift zone, the Koae fault zone, and the Hilina Pali (Fig. 2). This study examines the Koae fault zone, where seismicity was concentrated during the December, 1965, activity. The Koae is a east-northeast trending series of en echelon cracks and fault scarps, which merges with the east and southwest rift zones of Kilauea. Graben-type faulting is typical in the eastern Koae fault zone, while north facing scarps with vertical offsets up to 20 meters predominate in the central and western part of the fault zone (Duffield, 1975). Deformation and earthquake distribution studies have suggested that the southwest rift zone, Koae fault zone, and east rift zone act as tear-away zones separating the mobile south flank of Kilauea from the stable northern part of the volcano (Fiske and Kinoshita, 1969; Koyanagi et al, 1972, Duffield, 1975; Swanson et al, 1976). The stability of the northern flank of Kilauea is attributed to the buttressing effect of Mauna Loa Volcano to the north (Swanson et al, 1976).

The magnitude and extent of ground cracking that accompanied the December 1965 earthquake swarm may well have exceeded any that has taken place in the the past 100 years in the Koae - upper east rift region (Fiske and Koyanagi, 1968). Prior to this event, substantial earthquake activity located in the Koae had been recorded in May, 1938, December, 1950, and May, 1963 (Jaggar, 1938; Finch, 1950; and Kinoshita, 1968). The most recent activity related to the Koae took place in May, 1973, when an earthquake swarm and eruption occurred in the Koae and upper east rift region (Unger and Koyanagi, 1979). These episodes are similar to the December, 1965, activity, in that harmonic tremor, summit deflation, and surface ground cracking accompanied each earthquake swarm.

CHRONOLOGY OF EVENTS

The following sequence of events is a composite chronology of events reported by Fiske and Koyanagi (1968). All times are Hawaiian Standard Time.

At approximately 19:00, December 24, both harmonic tremor and a swarm of local earthquakes were first recorded on seismometers located near Kilauea's summit. Summit deflation was also apparent at this time, determined from the deflection of tiltmeters at Uwekahuna (Fig. 3). A party from HVO observed a bright glow and heard the roar of fountaining from a location close to Aloi Crater, at 21:00 (see Fig. 2). Actual fountaining could not be seen due to the rain and copious clouds of sulfur fume from the eruption. The time 21:30 is an approximation for eruption commencement. Cracks in the Chain of Craters Road, near Aloi Crater, had formed prior to the observation party's arrival at 21:45. Several cracks east of Pauahi Crater and near the intersection of the Ainahou Ranch Road and the Kalanaokuaiki Pali were also observed to have formed at this time. The Ainahou Ranch Road crack widened to 1 meter following a large earthquake at 21:45. Earthquake activity continued to increase through this time period.

Maximum intensity of the eruption in Aloi Crater occurred between 21:45 and 22:05, when the glow and roar of the eruption increased substantially. Maximum tremor amplitude was also recorded at this time, correlating with high levels of fountaining. Crack growth along the Chain of Craters Road reached maximum displacement, approximately 1.5 meters, at 23:00. Displacement was generally right lateral slip, with rare vertical offset downdropped to the southeast.

At 24:00, the observation party was able to view Aloi crater, and noted the eruption there was essentially over. However, a continued glow to the east and later reconnaissance showed fissure outbreaks extending 3.3 kilometers northeast of Aloi Crater to the cinder-lava cone Kane Nui O Hamo (see Fig. 2). By 04:00, December 25, lack of visible eruption signs indicated the eruption had terminated. It was at this time that the frequency of earthquakes was greatest, almost 90 per hour as recorded by a summit seismometer. The period of most intense earthquake activity was between 03:00 to 14:00, December 25, a full ten hours following the end of the eruption. Harmonic tremor and summit deflation also continued long after the eruption had ended. Deflation continued until 12:00, December 25, and tremor until 16:00, December 26. The cracks along the Chain of Craters Road attained maximum growth rate at 04:00, December 25.

A 0.7 meter wide crack was observed at the Hilina Pali Road, where it intersects the Kalanaokuaiki Pali, at 08:15, December 25. At 08:40 an earthquake jolted the area, and the crack opened to 1.7 meters. By the morning of December 27, the crack had opened to it's full extent of 3.3 meters. In general, there was a westward migration of crack activity with time, from the Chain of Craters Road near Aloi Crater to the intersection of the Hilina Pali Road with the Kalanaokuaiki Pali. Earthquake activity diminished and the frequency plot (Fig. 3) followed a hyperbolic decay curve to the end of the crisis (Fiske and Koyanagi, 1965).

DATA AQUISITION AND REDUCTION

Earthquakes during the December 1965 swarm were recorded by twelve permanent seismographs, and one portable instrument, maintained by HVO. The majority of the seismograph stations had short period instruments to accomodate the high level of microearthquake activity on Hawaii.

The locations of the permanent stations fall into two groups; instruments lying within the immediate vicinity of Kilauea Volcano (Fig. 2), and those instruments at greater distances from the volcano lying along the periphery of the island (Fig. 1). Each outer station had it's own independent clock and paper records while the inner stations were hard-wired to a common clock and recorded at HVO. WWVH was recorded twice daily at all stations, thereby establishing a criteria for any clock corrections due to drift. Either optical, pen, or smoked paper recording was used (Fig. 4). All permanent stations had single component vertical instruments, except for the three stations HIL, KLK, and USZ, which had three component instruments.

A portable, short-period, high-gain strip chart seismograph was operated for periods of several hours per day in several locations during the highest levels of earthquake activity (Fiske and Koyanagi, 1968). The instrument had two components (vertical and horizontal) recorded on strip chart paper with WWVH time code.

Seismograms were made available for this study by HVO. In general, earthquakes having a signal duration of 40 seconds or greater were reduced and analysed. Signals from earthquakes with coda less than 40 seconds were usually not strong enough to be read on a representative number of seismographs for location purposes. Reduction consisted of reading P and S wave arrival times, signal durations, and first motions. This information was then input into the earthquake location program HYPO71 (Lee and Lahr, 1975) on the Hawaii Institute of Geophysics Harris computer system. Problems in obtaining a standard time reference were solved as explained in Appendix A.

The location program uses a step-wise multiple regression, to determine the hypocenter and it's origin time. Station delays used in this study for the 1965 seismograph network were determined empirically by HVO (F. Klein, personal comm., 1980). Although several crustal models for the the island of Hawaii have been proposed (Eaton, 1962; Ryall and Bennet, 1968; Hill, 1969; Crosson and Koyanagi, 1979), the following HVO velocity model was used (Koyanagi et al, 1978) in order to maintain continuity with the HVO epicenter determinations;

LAYER	VELOCITY (km/s)	DEPTH	THICKNESS
1	1.8	0.0	0.8
2	3.1	0.8	1.4
3	5.2	2.2	5.8
4	6.8	8.0	5.5
5	8.25	13.5	

The location program allows the user to specify any latitude, longitude, and depth as the trial hypocenter. It is at this point that the location program initiates it's search for the final hypocenter. If a trial epicenter is not given by the user, the program defaults to a trial epicenter approximately located at the seismograph station which recorded the earliest arrival time from the earthquake in question (Lee and Lahr, 1975). It is accepted that much of the seismicity recorded on the island of Hawaii is a consequence of magmatic processes associated with Kilauea and Mauna Loa Volcanoes (Koyanagi et al, 1972; Estill, 1979). Based upon this assumption of local earthquake origin and also the small S-P time differences the program was allowed to default to a trial epicenter beneath the station with the earliest arrival time. A trial focal depth of five kilometers was chosen on the basis of several trial depth models attempted by the author (see Appendix B). Studies also indicate a five kilometer focal depth is a reasonable approximation for the average Kilauea "volcanic" earthquake (Koyanagi et al, 1972).

Contour mapping of RMS time residuals for several earthquakes was done in order to provide a better understanding of earthquake location precision. This procedure involves forcing solutions to locations adjacent to the determined hypocenter, and obtaining RMS time residuals for these points using the original set of arrival time data. RMS values were determined for a square grid with solutions spaced a kilometer apart from each other in both vertical and horizontal planes.

Earthquakes having low RMS values, small horizontal and vertical errors, and recorded on a representative number of stations (usually greater than or equal to 5), had contours which were closely packed around the determined hypocenter (Fig. 5). Closely spaced contours are equivalent to large RMS gradients, which in turn are analagous to tight, well-constrained solutions. Widely spaced contours or small RMS gradients, such as in the case of earthquakes located outside of the seismic network (Fig. 6), are typical of earthquakes which are not as well located. Fortunately, the majority of earthquakes analysed in this study occur well within the instrument net so there is good geometric control on the locations.

In the case of earthquakes located outside the net, elongation of RMS contours can provide us with useful information pertaining to station coverage. The principal axis of the RMS contour figure points toward the highest concentration of seismic instruments. It is along this azimuth that earthquake location precision is lowest. Elongation of contours to the southeast are due to lack of instrument control close to and surrounding the outer hypocenters. The determined hypocenter for Fig. 6 does not fall at a minumum RMS value because unweighted arrival times were used in the RMS mapping procedure. All earthquakes located by the location program used weighted arrival times, based both on user's input and program determined statistics.

In general, lack of precision in earthquake location can be attributed to bad arrival time picks, timing errors, and inadequate station coverage (Ward and Gregersen, 1973). Poor locations have been eliminated from the final earthquake data set used for seismicity plots. Only earthquakes having RMS values less than or equal to 0.3 seconds, horizontal and vertical errors less than or equal to 1.5 kilometers, and read from 5 or more stations were plotted.

SEISMICITY IN SPACE AND TIME

Epicenters of earthquakes have been located and plotted for the time period 12:00 on December 25 to 08:00 on December 30, 1965 (Fig. 7). Seismograph stations on Kilauea Volcano and major structural features of the volcano have also been located on the epicenter plots.

A broad NE-SW trending ellipsoidal pattern of earthquakes is centered within the Koae fault zone (Fig. 7). The epicentral region is terminated to the east by the east rift zone, and the western extent of these earthquakes fade out a few kilometers east of the southwest rift zone. Seismicity to the west of the Koae earthquake group is very low, with a few earthquakes located on the southwest rift zone and further west in the Kaoiki fault zone. Seismicity in the Kaoiki fault zone may be related to the stresses generated within Kilauea because of loading by the Mauna Loa volcanic system (Koyanagi et al, 1972).

Earthquake activity during the period analysed is absent north of the east rift zone. This region is considered to be the stable north flank of Kilauea, undergoing no present deformation (Koyanagi et al, 1972; Swanson et al, 1976; Ryan et al, 1981).

Earthquake activity in the summit area is low. The summit earthquakes that are observed probably represent deformation due to reinflation of the volcano's magma chamber following the deflation episode of December, 1965. Deflation is a direct consequence of magma withdrawl from the summit reservoir to the rift zones (Eaton, 1962; Moore and Koyanagi, 1969). The movement of magma from the summit area into the east rift zone during the December, 1965, activity can be inferred by summit deflation, strong harmonic tremor recording on upper east rift seismographs, and the eruption of lava at Aloi crater (Fiske and Koyanagi, 1968). Scattering of earthquakes on the south flank of Kilauea and further out to sea is also characteristic of Kilauea seismicity (Koyanagi et al, 1972). The seismic activity of late December, 1965, is similar to that of other seismic episodes on Kilauea, except for the unusually large concentration of earthquakes in the Koae fault zone. This region warrants great interest, and the remainder of this paper will focus on the Koae.

Hypocenters have been displayed in cross sections both parallel and perpendicular to the N70E trend of the Koae fault system. A width of 6 kilometers was chosen for the cross section parallel to the Koae (Fig. 8). An analogous plotting scheme was used for contouring of hypocentral concentration (Fig. 9). These plots contour the density of earthquakes per cubic kilometer at a contour interval of 1 earthquake. The range of focal depths is between 0 and 9 kilometers. A prominent clustering of earthquakes occurs at shallow depths (0-3 km.) in the eastern Koae, and there is a second grouping of deeper events (4-7 km.) in the central and western Koae. A 30 degree, southeasterly dipping trend of earthquakes can be observed in the central and western Koae (fig. 10). A width of 3 kilometers was chosen for the cross sections taken normal to the Koae.

Earthquakes located beneath Kilauea rift zones generally do not exceed 5 kilometers in depth, while focal depths as great as 10 kilometers are found to the south of the rifts. One possible explanation for this is that magma storage reservoirs, unable to support brittle fracture, exist at a depth between 5 and 10 kilometers beneath the rifts. Moving away from the rifts, and likewise the magma, cooler material is present at these depths and capable of fracture (R. Koyanagi, personal comm., 1981). This suggestion might be a reasonable explanation for the east to west variance of focal depth distribution in the Koae fault zone. The absence of earthquake occurence between a 4-7 kilometer depth in the east Koae might define an intrusive body of magma emplaced during the initial stages of the December activity. Missing from this data set are the times and locations of the first 16 hours of earthquake activity, lost due to the masking effects of the high earthquake and tremor activity. These times and locations would have provided evidence for or against magma migration into the eastern Koae.

Unger and Koyanagi (1979) suggest that during the May 5, 1973, Kilauea upper east rift zone eruption, magma was intruded from the east rift zone into the eastern Koae fault zone, and the effects (earthquakes) of this intrusion were propagated further into the Koae. The westward migration of fissures and earthquakes, horizontal and vertical ground surface changes and ground tilt before, during, and after the episode supports this suggestion (Unger and Koyanagi, 1979). Self-potential studies exhibit anomalies at the intersection of the Koae fault system with the east rift zone, which have been interpreted to represent shallow intrusions into the Koae (Jackson and Sako, 1979). A detailed gravity survey shows that Koae faults are partly filled by a dense material, possibly dikes (Duffield, 1975). The distribution of earthquakes, the continuation of harmonic tremor and summit deflation 10 hours after the termination of the eruption, and the previously mentioned studies suggest an intrusion into the eastern Koae. Fault plane solutions also support a magmatic intrusive event, and will be discussed later in the text.

The times of earthquake rupture were examined for any temporal progressions. No obvious progressions were observed through the time period studied.

MAGNITUDES AND B VALUES

Magnitudes were estimated from signal duration using the empirical HVO formulas;

$$M = -5.00 + 3.89 \text{ Log } (t), \text{ (t less than 210 seconds)}$$

$$M = -0.705 + 2.026 \text{ Log } (t), \text{ (t greater than or equal to 210 sec)}$$

where M is magnitude based on the Richter scale (Richter, 1958), and t is signal duration in seconds (Koyanagi et al, 1978). The inability to record accurate amplitudes, due to lack of dynamic range (clipping) and close line spacing on the paper records, necessitated the employment of signal duration magnitude determination. Signal duration is the time between the first arrival of the seismic wave to a point where the signal's amplitude is equivalent to the background noise prior to the first arrival. Approximately 20 durations could not be accurately measured, and approximations were made.

Amplitude magnitudes of 22 earthquakes, which overlapped the later portion of this study's earthquake set, were determined by R. Koyanagi (personal comm., 1981) at HVO. Duration magnitudes calculated for the same 22 earthquakes by this study were compared to the HVO amplitude magnitudes. In general, this study's duration magnitudes were larger than the HVO amplitude magnitudes, averaging 0.8 units difference. Possible explanations for the higher duration magnitudes are;

1. this author's technique for measuring signal duration may differ from that of other investigators (Hawaiian Volcano Observatory signal durations for these events were not available,
2. the duration formulas used may not be appropriate

used to record the late December, 1965 earthquakes (duration formulas were derived using earthquakes which occurred during 1975, 1976).

Caution should be exercised in interpreting these magnitudes individually. However, because signal durations were measured in a consistent manner, any spatial or temporal magnitude trends should not be effected by the high readings.

Most magnitudes are between 2 and 3. The largest magnitude recorded was a 4.4, and the smallest locatable event analysed had a 0.1 magnitude. The magnitude distribution was examined both temporally and spatially, but no trends could be established.

No discernible large main shock occurred during the period studied. The December, 1965, seismicity can aptly be termed an earthquake swarm (Mogi, 1963) because of the absence of a predominant earthquake, and because of the intensely fractured volcanic structure of Kilauea. Earthquake swarms are typical of volcanic environments (Koyanagi et al, 1972; Klein et al, 1977).

A b value of $0.94 \pm .07$ was determined for the complete set of earthquakes analysed, using the maximum likelihood method (Aki, 1965);

b = ~~2.3026~~ 0.434/(M-Mi)

M equals the average magnitude, and Mi equals the low magnitude cut-off (2.7). This method was chosen over the linear least squares fit to the Gutenberg-Richter frequency magnitude relation;

$$\text{Log } N = a - bM$$

where N equals the number of events larger than or equal to M (magnitude), because of the possible error involved in using an unweighted least squares fit (Carter and Berg, 1981).

Magnitudes were grouped into two different sets, using the focal depths of the earthquakes as a means for seperation. The two groups had depth intervals of 0.0 to 2.0 kilometers and 3.0 to 8.0 kilometers. A higher b value of 1.0 $\pm$ .23 was determined for the shallow set of events, compared to a b value of .89 $\pm$ .07 for the deeper set of events. Due to the lack of sufficiently large enough sample sets for the two groups of events, the statistics of these b values were poor, and should be treated with caution. The relationship of the b values to the tectonic implications of the earthquake swarm will be discussed later.

FOCAL MECHANISMS

Composite focal mechanism solutions were determined for earthquakes situated in the Koae fault zone (Fig. 11 and Fig. 12). Shallow earthquakes in the eastern Koae are characterized by near vertical faulting striking to the north. Faulting in the western and central Koae is predominatly normal, with a right lateral strike-slip component. N60E-N85E trending nodal planes were chosen as the strike of major faulting in the central and western Koae, based on the east-northeast trend of faults and cracks of the Koae fault zone (Duffield, 1975; Swanson et al, 1976). A southeasterly dip of 30 $\pm$ 17 degrees has been determined for these nodal planes. The depths of these earthquakes are between 4 and 7 kilometers.

Traditional focal mechanism techniques for body waves utilizing lower focal sphere, equal area net projection were used for this study (Brumbaugh, 1979). The impulsive first arrivals and the localized concentration of many earthquakes enabled the application of a composite focal study. HVO records indicate the distant station NBY (Fig. 1), in use at the time of the activity, had reversed polarity. Due to the presence of emergent first arrivals, readings from this station were not used in any of the focal solutions. All other polarities were consistent.

Previous focal mechanism studies suggest a variety of processes operative within the Kilauea Volcano vicinity; rift dilation (Ando, 1979; Furumoto and Kovach, 1979; Crosson and Endo,1981), south flank compression (Endo at al, 1979), and strike slip faulting between Mauna

Loa and Kilauea volcanoes (Endo et al, 1979).

During the December 1965 activity, the central and western Koae fault zone were undergoing both extension and strike-slip faulting. Displacement of the south flank away from the stable north flank of Kilauea has been suggested in previous studies (Swanson et al, 1976; Koyanagi et al, 1972; Fiske and Kinoshita, 1969) and fault plane solutions from this study agree with this concept.

It was previously noted that a southeasterly dipping trend of earthquakes existed in the Koae. The dip of this trend, and the mean dip from the fault-plane solutions, is approximately 30 degrees. Slippage along this seismic trend may define a diffuse plane upon which displacement of the south flank may occur (Fig. 13). This plane is compatible with the southerly dipping, low angle fault plane determined for the 1975, Kalapana, Hawaii earthquake (Ando, 1979; Crosson and Endo, 1981). Ando (1979) suggests that the fault plane of the Kalapana earthquake coincides with the boundary between the old ocean floor and the base of the volcano. The depth of this boundary is 10 kilometers, approximately 4 kilometers deeper than the seismic plane defined by this study. Ryan et al (1981) seismically define the base of the volcanic edifice in the Kilauea summit region to be at a depth of approximately 6 kilometers. This depth is consistent with the 4 to 7 kilometer depth of the seismic zone, determined by this study to underlie the Koae fault system. Swanson et al (1976) suggests that the base of the mobile south flank may be several kilometers thick rather than a single plane of dislocation, which is consistent with this study's results. Other possible boundaries upon which seaward displacement of the south flank occurs include a Kilauea-Mauna Loa contact (D. Epp, personal comm., 1981), and a weak low velocity layer at a 10 to 12 kilometer depth (Crosson and Endo, 1981).

It should also be pointed out that about 1.47 meters of right lateral offset was recorded along cracks that crossed the Chain of Craters Road near the site of the eruption (Fiske and Koyanagi, 1968). The relation of this offset and the strike-slip movement in the central and western Koae is presently unknown.

The least principal axis of stress in this area has a direction approximately perpendicular to the Koae. The intermediate axis of stress is coincident with the trend of the Koae and the rift zones, hence fractures striking parallel to this axis, and extension normal to it would be expected. North striking faults implied by the mechanisms in the eastern Koae present an anomaly to this N-S extension. Perhaps initial faulting, due to the intrusive magmatic event mentioned earlier, reactivated old faults or formed new cracks. An east-west migration of magma from the east rift zone into the Koae might have shifted the least principal axis of stress from N-S to E-W. Thus, N-S striking fractures parallel to the intermediate axis of stress would be a reasonable assumption. Later movement along these N-S striking faults would explain the fault plane solution pattern found for the eastern Koae.

RELATIONSHIP OF b-VALUES TO TECTONIC IMPLICATIONS

It has been determined that b values vary inversely to stress, both experimentally and for the earth (Scholz, 1968). The computed b value of .94 ± .07, for the complete set of earthquakes analysed, falls within the mid to upper b value range for earthquakes having a tectonic origin, compared to higher b values characteristic of a volcanic origin (Asada et al, 1951; Shimozuru, 1971). At first glance, a tectonic origin for the December, 1965 earthquake swarm is clearly not the case. The earthquakes analysed occurred at shallow depths in the volcanic pile of active Kilauea Volcano, and were accompanied by a volcanic extrusive and intrusive event, harmonic tremor, and summit deflation, certainly implying a volcanic origin for the seismicity. However, it should be recalled that a substantial amount of south flank displacement occurred during the earthquake swarm, and this movement was tectonic in nature, possibly being a secondary effect of forceful magma intrusion. The low b value determined for the deeper set of events also suggests a tectonic origin for earthquakes located along the determined plane of slippage in the central and western Koae at a 4 to 7 kilometer depth. The higher b value calculated for the shallow set of events, primarily located in the eastern Koae, may be a result of an intensely fractured environment generated by the inferred intrusive event. It appears that the December, 1965, earthquake swarm had both volcanic and tectonic origins, and that the computed b value of 0.94 ± .07 for the entire set of events is a reasonable one.

CONCLUSIONS

The Kilauea earthquake swarm of late December 1965 was concentrated within the Koae fault zone. Extensive cracking and faulting, and a small east rift eruption accompanied the earthquake swarm (Fiske and Koyanagi, 1968). The earthquakes and fracturing were a consequence of extension along the Koae, and subsequent seaward displacement of the south flank of Kilauea. Continuous inflation (Swanson, 1972) of Kilauea builds up a hydrostatic head of magma that eventually is relieved by either a surface eruption or subsurface intrusion. During the time period 1961-1965, the volume of lava extruded was very small compared to preceeding and subsequent eruptions (Macdonald and Abbott, 1970; Dzurisin et al, 1980). A large build-up of pressure took place over this time period, with little relief from large-scale eruptions which would act as safety valves for pressure release. The ultimate release of stress was presumably accommodated by displacement of the south flank, chiefly along the Koae. The displacement was an effect of dike intrusion in the upper east rift and eastern Koae. This study concurs with other authors′ beliefs that the Koae fault zone, in addition to the southwest and east rift zone, comprises a tear away zone where seaward displacement of the south flank away from the stable north flank of Kilauea occurs (Fiske and Kinoshita, 1969; Koyanagi et al, 1972; Duffield, 1975, Swanson et al, 1976).

Examination of the spatial distribution and focal mechanisms of the earthquakes reveals several trends. The first is an absence of earthquakes between 4 and 7 kilometers depth in the eastern Koae which may outline an intrusive magma body emplaced during the initial portion of the swarm. The presence of vertical faulting directly above this region is consistent with the idea of an intrusive event. Secondly, there exists a 30 degree, southeasterly dipping zone of earthquakes in the central and western Koae, supported both by fault plane solutions and spatial distribution of earthquakes in depth. A plane upon which seaward displacement of the south flank of Kilauea can take place has been suggested for this feature.

APPENDIX A

EARTHQUAKE SOLUTIONS

Single line outputs of individual earthquakes are displayed for all earthquakes analysed in this study. Symbol abbreviations are as follows; DATE=date of earthquake: year, month, and day, ORIGIN=origin time: hour, minute, and second (HST), LAT N=latitude north, of epicenter in degrees and minutes, LONG W=longitude west, of epicenter in degrees and minutes, DEPTH=focal depth in kilometers, MAG=duration magnitude of earthquake, NO=number of stations used in location, GAP=largest azimuthal separation in degrees between stations, DMIN=epicentral distance to nearest station, RMS=root mean square of time residuals in seconds, ERH=standard error of the epicenter in kilometers, and ERZ=standard error of the focal depth in kilometers.

DATE	ORIGIN	LAT N	LONG W	DEPTH	MAG	NO	GAP	DMIN	RMS	ERH	ERZ
651225	13 4 51.89	19 17.20	155 14.54	1.10	3.35	5	217	9.9	0.48	16.6	8.4
651225	1313 31.04	19 22.00	155 17.27	5.00	3.16	4	251	2.5	0.04	0.0	0.0
651225	1324 47.36	19 18.92	155 19.19	2.35	2.30	5	246	7.6	0.04	0.4	6.0
651225	1329 23.52	19 19.64	155 16.57	7.65	1.92	4	303	5.2	0.02	0.0	0.0
651225	1330 7.07	19 21.11	155 18.12	2.06	2.63	4	272	4.6	0.08	0.0	0.0
651225	1338 59.87	19 19.15	155 18.79	6.77	2.53	6	244	7.8	0.02	0.7	0.2
651225	1346 4.43	19 18.45	155 14.48	5.70	3.83	4	304	7.7	0.12	0.0	0.0
651225	1353 26.60	19 20.60	155 19.67	5.69	1.57	7	158	7.4	0.12	1.0	0.6
651225	14 3 17.61	19 19.96	155 18.72	5.41	2.61	6	176	6.7	0.03	0.4	0.3
651225	1420 43.11	19 18.75	155 11.30	1.08	1.23	4	278	10.5	0.14	0.0	0.0
651225	1430 24.77	19 18.14	155 18.45	5.69	0.67	6	264	9.0	0.08	2.5	0.5
651225	1431 10.95	19 20.55	155 14.48	9.53	3.86	5	258	4.2	0.05	3.1	0.8
651225	1440 13.74	19 21.96	155 17.12	4.00	3.67	5	184	2.3	0.25	3.9	3.1
651225	1448 1.75	19 18.90	155 19.95	3.65	2.77	4	244	6.3	0.00	0.0	0.0
651225	15 1 57.10	19 21.22	155 18.88	6.55	2.59	6	154	5.7	0.13	1.4	1.1
651225	1522 42.30	19 20.80	155 16.80	5.94	1.23	5	189	0.3	0.08	2.7	2.2
651225	1524 44.12	19 21.62	155 15.06	0.81	1.23	4	269	2.1	0.04	0.0	0.0
651225	1527 30.64	19 20.22	155 15.96	2.43	1.23	6	268	1.6	0.02	0.5	0.5
651225	1528 36.13	19 20.80	155 16.80	3.80	2.86	6	128	0.3	0.11	2.2	2.3
651225	1529 11.29	19 21.49	155 18.75	10.08	2.39	4	141	3.9	0.03	0.0	0.0
651225	1530 17.46	19 20.93	155 17.11	1.24	2.87	6	206	0.8	0.14	3.0	2.3
651225	1534 2.12	19 22.50	155 16.00	5.00	1.57	4	180	0.3	5.30	0.0	0.0
651225	1557 0.07	19 22.50	155 16.00	1.24	3.62	9	90	0.3	0.25	1.2	0.5
651225	16 1 6.01	19 20.56	155 17.41	0.00	2.60	4	251	1.3	0.34	0.0	0.0
651225	1623 18.89	19 21.95	155 17.97	5.00	1.76	5	145	3.7	0.14	2.2	2.0
651225	1638 20.43	19 24.28	155 18.01	13.24	4.28	5	144	38.5	0.36	4.0	8.8
651225	1640 53.04	19 22.50	155 16.00	5.00	2.89	3	180	0.3	1.24	0.0	0.0
651225	1653 42.99	19 17.39	155 20.53	0.27	3.06	5	164	7.1	0.15	2.4	22.6
651225	17 5 55.12	19 19.90	155 14.69	3.95	1.50	4	300	5.1	0.03	0.0	0.0
651225	1710 36.13	19 23.58	155 9.97	3.00	3.80	4	334	10.6	0.23	0.0	0.0
651225	1715 26.06	19 20.21	155 15.59	3.24	1.84	5	206	4.1	0.11	4.6	2.1
651225	1718 20.95	19 18.49	155 18.76	5.00	2.46	6	230	8.6	0.09	1.3	0.5
651225	1726 32.82	19 21.98	155 17.00	5.00	3.06	6	185	2.1	0.12	1.3	0.8
651225	1728 45.41	19 19.37	155 18.65	5.19	2.62	6	240	7.4	0.10	1.5	0.6
651225	1733 6.42	19 15.56	155 16.01	5.00	2.61	5	314	12.6	0.27	13.0	3.0
651225	1733 7.96	19 21.56	155 16.00	3.94	2.61	7	160	1.6	0.11	1.1	0.6
651225	1740 13.49	19 21.02	155 14.28	2.70	1.20	5	244	3.8	0.17	21.9	13.8
651225	1741 16.58	19 21.10	155 18.55	7.62	1.89	6	196	5.2	0.07	1.1	0.4
651225	1744 40.08	19 29.85	155 17.10	1.54	2.06	3	320	9.1	0.42	0.0	0.0
651225	1746 1.72	19 21.18	155 18.47	3.27	1.95	3	195	5.0	0.00	0.0	0.0
651225	1751 3.27	19 21.70	155 18.84	4.98	3.21	9	145	5.3	0.13	0.8	0.5
651225	1758 15.56	19 22.85	155 18.44	7.15	3.35	4	186	4.5	0.01	0.0	0.0
651225	18 8 1.37	19 20.52	155 14.86	3.00	2.87	3	311	3.9	0.02	0.0	0.0
651225	1812 24.94	19 18.22	155 17.56	6.90	2.93	8	204	8.2	0.10	1.1	0.4
651225	1815 36.74	19 16.60	155 14.86	1.47	1.23	6	275	10.9	0.15	2.8	1.4
651225	1821 6.40	19 21.96	155 21.35	4.00	2.67	7	262	9.3	0.23	2.4	1.1
651225	1822 38.23	19 23.92	155 17.10	3.00	2.65	3	222	1.8	0.04	0.0	0.0

651225	1829	36.79	19	22.81	155	15.45	0.76	1.23	4	262	1.1	0.02	0.0	0.0
651225	1830	1.15	19	19.68	155	18.31	5.00	2.34	8	185	6.6	0.16	1.6	1.0
651225	1831	18.26	19	22.83	155	18.00	5.00	2.23	6	140	3.8	0.16	1.4	1.1
651225	1833	7.88	19	20.04	155	17.69	4.00	2.40	4	236	5.4	0.13	0.0	0.0
651225	1835	15.36	19	18.04	155	13.86	5.00	1.69	3	318	8.8	0.12	0.0	0.0
651225	1839	17.66	19	16.95	155	12.85	4.78	3.02	6	223	11.4	0.11	3.4	2.1
651225	1849	33.45	19	19.74	155	16.77	0.23	2.02	5	257	5.1	0.04	1.2	1.2
651225	1854	59.68	19	17.04	155	16.00	5.47	2.50	5	293	9.9	0.08	0.0	0.0
651225	1859	46.64	19	22.50	155	16.00	3.27	3.61	3	202	0.3	2.32	0.0	0.0
651225	19 5	10.60	19	20.18	155	13.88	0.00	2.92	7	212	5.4	0.20	1.9	1.2
651225	1912	37.70	19	17.57	155	15.00	6.94	2.73	4	298	9.0	0.13	0.0	0.0
651225	1915	56.96	19	21.60	155	17.94	2.99	1.23	5	187	3.9	0.02	0.3	1.2
651225	1916	9.88	19	21.31	155	17.94	3.30	2.65	4	197	4.1	0.04	0.0	0.0
651225	1919	0.07	19	16.69	155	18.80	5.52	2.55	5	316	11.7	0.00	0.0	0.0
651225	1921	22.92	19	16.58	155	15.43	2.00	1.23	3	330	10.8	0.12	0.0	0.0
651225	1921	59.11	19	20.62	155	15.02	1.23	3.86	7	263	3.6	0.09	1.3	0.4
651225	1930	43.10	19	21.60	155	18.18	5.00	1.25	8	184	4.2	0.16	1.3	0.7
651225	1933	52.20	19	19.53	155	18.97	5.00	2.78	4	234	7.5	0.13	0.0	0.0
651225	1945	24.41	19	21.27	155	18.28	5.00	2.27	4	194	4.7	0.05	0.0	0.0
651225	1947	47.79	19	15.43	155	17.23	1.00	1.23	4	299	13.1	0.28	0.0	0.0
651225	1948	13.90	19	20.22	155	14.12	2.69	4.08	6	211	5.1	0.05	2.8	2.7
651225	1953	31.87	19	20.32	155	15.43	6.00	1.52	4	281	3.9	0.10	0.0	0.0
651225	1956	37.96	19	21.71	155	23.40	3.69	2.88	5	184	2.8	0.07	1.0	0.8
651225	20 2	19.44	19	19.43	155	14.86	3.00	2.76	8	210	5.8	0.19	3.0	1.7
651225	20 4	17.93	19	17.81	155	10.99	2.24	2.74	4	270	12.1	0.19	0.0	0.0
651225	20 6	29.30	19	22.33	155	16.74	1.93	1.74	4	166	1.5	0.01	0.0	0.0
651225	20 7	52.24	19	20.62	155	14.79	1.51	3.65	5	293	3.8	0.06	0.8	0.4
651225	2012	54.17	19	20.77	155	15.27	0.89	2.55	7	243	3.2	0.19	2.4	1.1
651225	2014	45.17	19	21.44	155	16.00	1.51	3.33	10	160	1.8	0.21	1.3	0.5
651225	2018	37.10	19	20.18	155	14.78	3.17	2.53	9	208	4.5	0.14	1.9	1.0
651225	2020	6.01	19	17.71	155	12.42	3.39	4.20	4	272	10.6	0.19	0.0	0.0
651225	2027	20.98	19	21.47	155	14.44	3.27	2.31	7	198	3.1	0.23	2.4	1.7
651225	2038	18.81	19	19.52	155	12.89	1.50	1.61	4	310	7.5	1.13	0.0	0.0
651225	2038	48.36	19	20.78	155	14.86	4.14	3.42	8	166	3.5	0.17	1.8	1.0
651225	2054	53.51	19	19.45	155	13.56	2.25	3.11	8	247	6.6	0.20	4.5	3.2
651225	2058	24.99	19	22.50	155	15.04	1.45	1.47	5	196	1.2	0.04	0.0	0.0
651225	2059	44.34	19	21.34	155	19.94	7.81	1.87	5	176	6.2	0.01	0.1	0.1
651225	21 2	55.51	19	17.41	155	15.38	0.68	1.23	5	270	9.3	0.26	17.6	81.5
651225	2110	42.38	19	18.99	155	12.89	2.22	1.14	8	260	7.8	0.16	2.1	2.1
651225	2119	16.29	19	21.34	155	14.09	1.06	1.92	8	221	3.0	0.14	1.0	0.6
651225	2123	1.78	19	21.14	155	14.06	3.66	1.94	10	243	3.3	0.21	2.7	1.1
651225	2137	18.84	19	19.16	155	18.66	6.09	2.47	8	179	7.7	0.10	1.1	0.5
651225	2140	14.10	19	20.02	155	14.67	0.36	2.45	8	227	4.9	0.23	2.2	1.2
651225	2145	24.27	19	20.78	155	14.46	5.03	0.75	9	204	3.9	0.17	1.6	0.8
651225	2150	12.69	19	18.48	155	15.94	3.37	4.11	10	209	7.2	0.16	1.7	1.7
651225	2158	40.91	19	23.00	155	15.55	3.52	3.44	11	113	1.3	0.28	1.5	0.9
651225	22 4	15.68	19	20.05	155	12.90	2.44	1.91	6	254	5.9	0.20	3.6	3.0
651225	22 6	5.62	19	21.40	155	13.46	4.01	2.11	5	296	3.3	0.05	2.0	1.1
651225	2223	4.61	19	19.45	155	14.45	3.71	2.36	7	211	6.0	0.26	5.7	2.8
651225	2225	11.83	19	21.00	155	16.00	5.72	2.69	6	261	2.6	0.07	1.2	0.3

651225	2234	31.01	19	18.62	155	15.43	3.70	2.80	5	261	7.0	0.12	4.2	1.5
651225	2246	46.14	19	21.19	155	14.83	1.54	1.89	6	292	2.9	0.09	2.0	0.6
651225	2248	10.09	19	18.78	155	18.48	2.73	2.38	7	193	8.1	0.07	0.8	0.7
651225	2250	58.92	19	21.09	155	15.24	2.22	3.36	7	205	2.7	0.11	1.4	1.7
651225	2256	48.53	19	19.07	155	16.00	4.81	3.16	6	207	6.1	0.13	2.7	0.9
651225	2310	36.97	19	19.53	155	17.42	5.86	1.84	7	250	5.9	0.10	2.4	0.5
651225	2314	26.02	19	22.50	155	17.67	5.00	2.78	6	190	3.1	0.17	1.9	1.0
651225	2328	35.57	19	19.97	155	13.22	1.86	3.56	9	214	6.5	0.09	0.8	0.4
651225	2333	59.40	19	21.90	155	16.12	2.25	1.06	5	233	1.0	0.29	4.0	6.1
651225	2334	39.15	19	19.11	155	18.42	5.00	1.12	5	247	7.5	0.07	1.7	0.9
651225	2335	33.28	19	23.04	155	12.87	0.04	4.17	4	292	5.4	0.43	0.0	0.0
651226	0 3	42.41	19	12.23	155	17.02	9.47	2.11	10	196	18.4	0.20	2.1	1.7
651226	0 6	59.39	19	18.89	155	17.38	2.11	2.05	4	261	7.0	0.07	0.0	0.0
651226	013	29.82	19	21.96	155	19.95	12.31	1.23	5	157	6.7	0.11	4.2	3.6
651226	013	37.02	19	20.72	155	14.48	6.00	2.74	6	245	4.0	0.03	1.0	0.3
651226	015	18.82	19	19.49	155	19.67	6.14	2.60	6	172	6.5	0.21	2.3	1.2
651226	016	28.34	19	17.74	155	18.72	2.27	2.75	6	270	9.2	0.18	2.9	95.1
651226	022	23.54	19	22.05	155	14.34	5.43	2.91	7	236	2.8	0.11	1.4	0.7
651226	026	49.53	19	21.06	155	14.43	5.00	2.64	8	202	3.6	0.17	2.0	1.3
651226	031	6.91	19	21.85	155	18.30	3.52	1.97	6	174	4.3	0.05	0.6	2.1
651226	032	54.63	19	19.08	155	14.31	4.29	3.61	9	175	6.7	0.18	1.8	1.1
651226	039	21.31	19	22.78	155	14.42	0.17	2.09	4	302	2.7	0.01	0.0	0.0
651226	046	41.61	19	19.51	155	17.53	6.83	1.30	6	225	6.1	0.07	1.9	0.6
651226	111	31.81	19	18.31	155	16.43	6.02	3.74	8	172	7.6	0.05	0.5	0.2
651226	116	20.52	19	22.50	155	11.11	6.41	0.87	4	316	8.4	0.04	0.0	0.0
651226	122	51.25	19	18.88	155	21.12	0.74	3.24	4	248	4.5	0.02	0.0	0.0
651226	127	48.81	19	20.65	155	16.00	6.41	1.86	5	320	3.2	0.04	0.4	0.1
651226	129	18.80	19	18.41	155	15.43	6.50	4.14	8	226	7.4	0.12	1.5	0.5
651226	140	30.29	19	19.70	155	16.45	2.29	1.94	5	263	5.1	0.06	2.0	29.3
651226	157	49.93	19	19.27	155	19.05	6.81	2.75	9	181	7.6	0.12	1.0	0.3
651226	2 1	40.68	19	17.49	155	18.15	7.40	1.74	4	274	9.9	0.03	0.0	0.0
651226	2 2	9.64	19	18.87	155	18.28	6.18	3.47	6	253	7.7	0.08	2.5	0.6
651226	213	35.46	19	19.64	155	13.82	3.01	3.05	6	255	6.3	0.27	3.8	2.8
651226	222	37.82	19	19.31	155	16.69	3.67	4.07	7	204	5.9	0.12	1.8	1.0
651226	230	12.30	19	21.34	155	16.00	5.00	2.35	8	236	2.0	0.16	1.4	0.5
651226	233	50.61	19	20.87	155	16.00	1.22	2.10	5	261	2.8	0.19	5.9	2.1
651226	254	32.88	19	17.30	155	15.92	8.46	2.13	4	233	9.4	0.03	0.0	0.0
651226	3 0	10.80	19	19.48	155	18.22	6.62	2.77	8	189	6.7	0.23	2.8	0.8
651226	313	54.76	19	21.83	155	14.37	3.22	1.60	6	194	2.9	0.24	4.8	4.8
651226	317	34.84	19	20.16	155	15.43	5.04	2.45	8	206	4.2	0.25	2.8	1.7
651226	343	2.59	19	22.66	155	19.38	9.43	2.69	4	191	5.9	0.03	0.0	0.0
651226	351	4.26	19	21.02	155	16.00	5.00	3.08	9	162	2.5	0.24	1.8	0.9
651226	4 9	42.99	19	20.76	155	11.29	4.18	3.25	9	219	8.6	0.19	2.0	1.5
651226	418	16.25	19	24.66	155	13.72	1.27	3.00	5	199	5.7	0.32	6.2	34.3
651226	430	15.03	19	20.87	155	18.03	4.78	2.42	7	210	4.7	0.15	1.4	0.9
651226	432	42.58	19	18.93	155	18.71	6.44	2.69	7	249	8.1	0.07	1.4	0.3
651226	435	33.16	19	21.00	155	14.86	7.00	2.14	4	345	3.2	0.10	0.0	0.0
651226	442	4.51	19	17.99	155	16.00	5.23	3.80	8	210	8.1	0.04	0.6	0.2
651226	449	58.27	19	20.55	155	16.80	2.21	1.69	6	242	3.8	0.26	0.7	2.0
651226	5 8	48.98	19	21.51	155	16.57	1.64	2.68	7	223	2.0	0.17	3.5	1.5

651226	520	28.51	19	20.30	155	19.16	2.17	2.45	5	213	6.9	0.24	0.8	1.0
651226	526	24.29	19	20.82	155	15.24	4.45	2.63	7	243	3.1	0.09	1.2	0.5
651226	531	5.73	19	21.26	155	18.56	1.90	1.80	6	191	5.1	0.17	1.4	1.6
651226	543	55.62	19	19.77	155	16.00	2.64	1.92	7	250	4.9	0.20	2.4	2.0
651226	544	48.18	19	18.28	155	13.77	2.16	3.58	7	217	8.5	0.10	1.1	0.9
651226	549	26.87	19	19.20	155	17.76	6.10	2.70	8	252	6.7	0.14	1.3	0.6
651226	553	58.79	19	18.14	155	19.44	6.18	2.24	8	188	7.7	0.07	0.7	0.3
651226	554	42.48	19	21.42	155	17.14	4.73	3.46	4	275	2.8	0.22	0.0	0.0
651226	610	38.70	19	21.02	155	17.07	1.62	4.12	11	186	3.3	0.29	1.9	0.8
651226	618	1.57	19	20.68	155	18.01	8.09	2.99	7	175	4.9	0.11	1.3	1.2
651226	619	53.23	19	18.08	155	18.59	5.33	2.46	5	265	9.1	0.02	0.9	0.2
651226	622	29.03	19	20.00	155	17.68	2.47	2.02	5	237	5.4	0.06	1.0	17.2
651226	632	48.82	19	19.61	155	18.26	5.00	2.96	8	238	6.6	0.18	1.5	0.8
651226	7 4	30.55	19	21.34	155	17.91	4.94	2.37	10	156	4.0	0.11	0.7	0.5
651226	711	23.39	19	20.47	155	16.01	7.00	2.70	3	320	3.6	0.03	0.0	0.0
651226	718	5.67	19	23.04	155	16.57	4.00	2.94	9	147	1.7	0.64	5.0	2.4
651226	721	47.46	19	21.20	155	17.86	2.31	3.03	5	202	4.1	0.17	3.7	2.7
651226	731	5.84	19	21.52	155	18.14	2.13	2.51	5	188	4.2	0.19	0.0	0.1
651226	737	28.76	19	21.51	155	15.46	1.27	1.23	3	358	1.8	0.02	0.0	0.0
651226	739	36.25	19	19.68	155	14.83	3.00	1.68	3	359	5.4	0.06	0.0	0.0
651226	745	14.54	19	20.65	155	18.68	4.61	2.39	7	208	5.8	0.17	1.6	1.0
651226	748	10.26	19	22.50	155	16.00	3.41	3.01	7	180	0.3	0.18	2.5	1.2
651226	755	56.75	19	20.98	155	17.27	5.00	3.43	7	182	3.6	0.16	1.5	0.7
651226	8 7	41.31	19	19.03	155	14.88	7.48	2.78	6	294	6.5	0.04	1.1	0.4
651226	826	12.42	19	21.38	155	15.88	7.00	2.48	3	321	1.9	0.00	0.0	0.0
651226	850	49.82	19	20.92	155	18.81	2.10	2.30	6	199	5.8	0.25	2.2	2.4
651226	929	37.23	19	20.26	155	14.75	0.00	2.33	4	294	4.4	0.11	0.0	0.0
651226	945	26.20	19	19.32	155	19.14	2.28	2.35	6	223	5.0	0.05	0.7	28.4
651226	946	7.67	19	13.00	155	16.00	3.00	2.75	3	316	17.3	0.08	0.0	0.0
651226	950	37.65	19	20.87	155	16.01	3.27	2.78	5	200	2.8	0.23	3.1	3.0
651226	1015	51.67	19	20.30	155	19.32	2.22	1.97	5	211	7.0	0.17	2.5	63.2
651226	1028	1.39	19	11.07	155	17.79	3.72	3.01	7	310	17.9	0.15	3.1	2.0
651226	1032	5.95	19	21.04	155	16.57	6.00	2.83	6	161	2.8	0.24	2.8	1.5
651226	1119	16.66	19	20.26	155	16.23	4.91	1.08	6	261	1.2	0.12	2.8	1.1
651226	1125	57.85	19	19.29	155	17.37	1.24	1.23	7	255	2.9	0.12	1.3	0.6
651226	1133	46.59	19	19.54	155	18.85	4.40	3.11	6	180	7.4	0.16	1.8	2.2
651226	1139	57.28	19	19.82	155	18.21	1.85	2.52	8	216	3.1	0.16	2.3	0.9
651226	1211	44.40	19	20.37	155	15.61	0.19	3.64	10	206	2.0	0.16	0.8	0.6
651226	1237	4.30	19	18.17	155	19.13	2.13	3.23	5	255	6.3	0.06	1.0	0.7
651226	13 2	20.21	19	20.24	155	16.70	0.36	4.23	9	244	0.8	0.21	1.4	0.5
651226	1314	6.71	19	16.74	155	19.39	16.64	4.06	4	297	9.4	0.08	0.0	0.0
651226	1323	50.51	19	19.27	155	17.37	4.71	2.34	8	255	2.9	0.16	2.0	1.4
651226	1346	34.92	19	20.81	155	16.45	4.85	2.78	8	239	3.1	0.08	0.7	0.4
651226	1352	9.71	19	16.21	155	16.00	6.25	1.23	7	299	11.4	0.21	3.8	1.3
651226	14 3	59.33	19	18.79	155	18.77	4.07	1.70	6	251	8.3	0.12	2.0	6.4
651226	14 4	47.64	19	16.51	155	20.15	5.68	3.30	9	262	8.8	0.19	2.6	1.0
651226	14 6	34.60	19	18.45	155	18.26	2.33	2.86	6	260	8.4	0.16	2.2	70.2
651226	1427	14.68	19	19.92	155	17.41	5.78	3.03	9	243	5.3	0.13	1.1	0.5
651226	1433	49.45	19	20.24	155	16.03	0.00	1.96	5	266	4.0	0.14	11.0	6.9
651226	1455	53.43	19	15.07	155	15.14	8.04	2.65	12	189	13.6	0.10	0.9	1.3

651226	15 4	49.74	19	17.24	155	16.55	1.52	2.44	4	288	9.6	0.05	0.0	0.0
651226	1516	12.27	19	20.03	155	19.15	5.22	3.15	8	220	7.2	0.03	0.3	0.3
651226	1523	44.86	19	18.47	155	16.57	6.89	2.65	7	276	7.3	0.08	1.4	0.6
651226	1542	19.84	19	18.60	155	17.22	5.26	2.34	8	267	7.4	0.11	1.3	2.9
651226	1628	1.02	19	20.07	155	16.00	7.43	2.24	6	269	4.3	0.18	4.7	1.5
651226	17 7	33.05	19	17.19	155	12.95	7.79	3.41	4	271	10.9	0.02	0.0	0.0
651226	1818	49.35	19	19.44	155	16.85	2.99	2.39	8	252	5.7	0.21	3.2	3.0
651226	1826	57.99	19	19.22	155	17.09	6.88	2.31	6	260	6.2	0.02	0.3	0.1
651226	19 1	58.92	19	18.36	155	16.57	6.99	2.07	6	277	7.5	0.11	3.6	0.9
651226	1912	14.43	19	19.32	155	18.76	6.07	2.64	6	240	7.6	0.07	1.3	0.4
651226	1936	10.87	19	19.65	155	18.25	4.53	2.26	6	238	6.5	0.07	1.0	3.0
651226	2020	53.81	19	19.40	155	14.47	2.14	2.11	12	212	6.1	0.17	1.1	0.9
651226	2031	39.09	19	20.53	155	17.86	5.00	3.35	11	170	4.9	0.19	1.1	1.0
651226	2039	43.84	19	21.72	155	15.28	1.06	3.36	11	193	1.6	0.14	0.6	0.3
651226	2041	25.99	19	21.47	155	16.00	5.00	3.47	5	254	1.7	0.14	91.2	90.5
651226	2057	35.78	19	19.99	155	17.68	6.00	2.52	5	237	5.4	0.22	3.9	6.9
651226	21 3	47.09	19	22.08	155	14.49	4.54	2.61	4	296	6.8	0.02	0.0	0.0
651226	2118	16.55	19	17.81	155	17.70	1.01	3.50	8	171	14.0	0.21	1.7	1.1
651226	2141	21.00	19	25.00	155	17.10	7.46	2.24	4	186	0.3	0.15	0.0	0.0
651226	2141	23.92	19	26.04	155	17.13	2.27	2.96	3	272	1.4	0.40	0.0	0.0
651226	2244	43.21	19	20.32	155	16.53	0.83	3.62	7	222	8.5	0.35	3.8	3.1
651226	2256	27.42	19	24.26	155	14.08	7.40	2.13	4	180	5.2	0.05	0.0	0.0
651226	23 9	56.35	19	13.06	155	21.22	0.26	2.65	8	184	13.7	0.21	1.8	0.8
651226	2313	6.49	19	28.02	155	23.96	2.91	2.28	4	204	3.5	0.05	0.0	0.0
651226	2320	15.60	19	18.75	155	14.23	6.18	2.78	5	303	7.3	0.01	1.1	0.1
651226	2320	37.39	19	20.21	155	17.72	1.54	2.60	5	232	5.1	0.07	1.5	39.3
651226	2338	22.87	19	24.46	155	17.10	1.87	1.99	4	161	0.8	0.16	0.0	0.0
651226	2345	40.86	19	19.55	155	18.96	5.68	2.12	4	233	7.5	0.05	0.0	0.0
651226	2348	48.34	19	18.22	155	16.01	7.00	1.77	3	328	7.7	0.01	0.0	0.0
651227	0 6	40.08	19	20.96	155	16.01	3.27	1.68	7	260	2.7	0.27	4.0	3.1
651227	0 9	15.77	19	20.15	155	17.64	5.00	2.76	8	234	5.1	0.25	2.4	1.9
651227	012	13.58	19	23.04	155	15.43	4.00	1.72	7	142	1.4	0.34	4.4	3.7
651227	015	25.63	19	21.42	155	16.37	7.00	2.45	3	297	2.0	0.02	0.0	0.0
651227	017	1.97	19	21.64	155	16.00	5.00	2.47	5	170	1.4	0.22	2.8	3.3
651227	020	16.00	19	19.15	155	18.96	3.08	2.96	9	243	7.8	0.21	2.0	1.2
651227	037	0.54	19	19.81	155	17.86	6.86	1.73	9	239	5.9	0.15	1.4	0.6
651227	038	24.66	19	19.55	155	17.62	8.00	3.27	4	247	6.1	0.13	0.0	0.0
651227	043	9.60	19	15.92	155	14.79	7.29	2.18	5	307	12.1	0.06	13.0	1.3
651227	053	6.73	19	21.32	155	15.06	2.09	1.66	7	178	2.5	0.14	1.3	1.6
651227	121	28.61	19	20.33	155	17.99	3.96	3.12	11	146	5.3	0.29	1.7	1.1
651227	126	7.12	19	19.36	155	18.81	4.34	2.79	9	183	7.6	0.20	1.7	1.0
651227	139	31.78	19	21.96	155	16.57	6.00	1.55	5	199	1.4	0.14	2.5	1.4
651227	214	26.20	19	19.08	155	16.00	7.57	2.69	5	278	6.1	0.10	5.9	1.4
651227	244	35.59	19	23.44	155	18.18	4.63	2.80	4	121	3.8	0.02	0.0	0.0
651227	258	37.71	19	21.99	155	17.04	3.93	4.18	10	132	2.1	0.14	0.8	0.6
651227	3 4	11.53	19	20.82	155	16.63	2.22	2.08	5	183	3.2	0.03	0.4	64.8
651227	4 2	53.60	19	21.67	155	17.10	5.00	1.01	6	167	2.5	0.33	3.2	5.2
651227	425	13.56	19	20.68	155	18.64	0.00	2.68	5	182	5.8	0.05	0.5	1.8
651227	518	9.01	19	20.30	155	19.82	7.00	3.21	9	161	6.1	0.26	2.2	1.0
651227	544	7.88	19	17.54	155	16.00	8.51	2.86	7	238	9.0	0.16	2.4	5.8

651227	556	23.87	19	20.04	155	18.38	8.31	2.99	6	194	6.2	0.07	1.1	1.2
651227	645	4.47	19	20.45	155	14.99	0.96	3.53	10	167	3.9	0.18	1.2	0.8
651227	711	10.99	19	21.65	155	18.32	0.00	0.97	6	164	4.5	0.10	0.9	3.2
651227	758	40.89	19	21.20	155	18.27	6.61	2.48	7	173	4.7	0.21	1.7	2.1
651227	826	54.34	19	19.76	155	18.68	1.17	3.14	5	231	6.9	0.15	3.3	19.0
651227	838	26.92	19	21.42	155	16.01	13.68	1.51	5	254	1.8	0.21	2.8	2.4
651227	858	45.79	19	21.75	155	12.68	5.60	1.24	6	193	4.7	0.20	3.4	1.6
651227	913	45.12	19	22.19	155	18.24	1.21	2.60	4	155	4.1	0.10	0.0	0.0
651227	920	44.56	19	17.97	155	16.57	6.00	3.16	8	231	8.3	0.24	3.9	1.5
651227	938	16.47	19	21.96	155	18.12	9.46	2.35	4	172	4.0	0.20	0.0	0.0
651227	940	9.12	19	20.53	155	17.83	5.00	2.85	8	186	4.8	0.16	1.2	2.9
651227	944	16.56	19	20.96	155	18.06	8.42	2.75	6	178	4.6	0.11	1.4	2.4
651227	952	24.51	19	17.75	155	17.24	8.39	2.97	7	278	8.9	0.19	4.3	8.0
651227	10 9	23.67	19	20.87	155	16.48	4.00	2.88	9	183	3.0	0.29	1.8	1.6
651227	1028	52.50	19	19.34	155	17.14	4.28	3.37	10	208	6.0	0.15	1.3	0.6
651227	1036	7.76	19	20.33	155	16.23	0.00	1.63	7	193	3.9	0.11	0.7	1.1
651227	11 0	26.55	19	20.69	155	18.85	3.49	3.29	11	181	6.1	0.21	1.3	0.7
651227	1142	54.11	19	20.51	155	16.00	1.47	1.39	3	264	3.5	0.15	0.0	0.0
651227	1235	0.58	19	17.26	155	19.91	5.65	2.80	5	309	11.8	0.07	2.8	0.4
651227	1242	34.68	19	20.90	155	16.00	5.00	1.35	7	183	2.8	0.24	2.4	2.0
651227	1249	59.33	19	20.45	155	18.13	0.98	2.38	8	187	5.3	0.11	0.7	0.6
651227	1340	54.35	19	21.10	155	16.44	3.57	3.39	12	142	2.6	0.17	0.9	0.7
651227	1345	10.14	19	20.65	155	18.24	6.33	2.53	9	183	5.2	0.13	0.9	1.1
651227	1459	22.49	19	19.02	155	18.53	5.44	3.07	9	214	7.7	0.10	0.7	0.6
651227	1523	50.72	19	14.43	155	20.79	5.00	3.26	14	178	11.5	0.18	1.1	0.8
651227	1553	24.89	19	20.79	155	18.72	3.46	2.42	7	179	5.8	0.17	1.6	8.8
651227	1620	1.67	19	18.17	155	13.59	9.15	2.92	8	308	8.8	0.13	2.6	2.5
651227	1645	40.10	19	21.07	155	13.87	3.24	2.84	10	186	4.3	0.17	1.2	0.9
651227	17 4	38.12	19	21.40	155	15.08	2.99	2.62	9	176	2.3	0.13	0.8	0.8
651227	1738	36.68	19	18.07	155	14.29	6.00	1.91	5	303	8.5	0.13	8.9	1.1
651227	1752	13.35	19	22.50	155	16.00	3.74	3.52	9	110	0.3	0.21	1.5	0.8
651227	1814	33.10	19	11.54	155	19.67	5.74	3.74	13	201	17.2	0.16	1.3	0.8
651227	1822	43.81	19	21.24	155	18.76	5.00	3.20	4	189	5.4	0.13	0.0	0.0
651227	1830	52.74	19	20.14	155	18.54	3.42	3.01	6	223	6.2	0.17	2.6	1.6
651227	1838	13.51	19	20.65	155	17.13	3.44	3.17	5	232	3.9	0.01	0.3	0.2
651227	1846	8.53	19	21.06	155	14.68	6.00	2.88	8	242	3.3	0.17	2.6	0.9
651227	1922	1.45	19	21.04	155	17.42	5.60	3.14	6	215	3.7	0.06	0.9	0.5
651227	2016	17.98	19	19.61	155	18.37	7.12	2.75	6	203	6.7	0.03	0.5	0.3
651227	2129	38.31	19	22.39	155	14.04	2.48	2.84	11	157	3.3	0.22	1.2	1.2
651227	2148	6.42	19	19.30	155	17.44	6.48	2.84	8	209	6.3	0.05	0.5	0.3
651227	2223	5.75	19	15.25	155	20.28	6.11	3.36	11	175	10.5	0.13	1.0	0.7
651227	2226	59.46	19	20.84	155	19.70	4.00	3.51	11	154	6.4	0.22	1.5	0.8
651227	2259	23.61	19	19.34	155	17.28	2.65	4.01	6	231	6.1	0.12	3.6	4.1
651227	2259	26.38	19	20.44	155	15.43	0.44	1.23	8	206	3.7	0.22	2.0	0.8
651227	2336	40.10	19	19.78	155	17.63	4.00	2.86	9	242	5.7	0.19	2.4	1.0
651228	0 4	32.29	19	21.36	155	19.20	1.31	2.78	6	166	6.8	0.24	2.9	5.3
651228	034	55.41	19	17.84	155	17.81	10.32	2.41	6	232	9.1	0.07	1.6	2.6
651228	1 1	1.89	19	21.59	155	16.58	2.15	4.41	13	137	1.9	0.13	0.6	0.4
651228	147	22.72	19	11.55	155	13.17	5.09	2.03	6	296	19.7	0.06	2.3	0.5
651228	154	52.05	19	25.00	155	16.56	1.70	2.44	9	87	0.8	0.17	1.1	0.5

651228	156	59.13	19	21.53	155	19.43	4.27	2.33	6	162	6.4	0.19	1.8	8.9
651228	2 6	53.85	19	17.08	155	9.66	3.00	1.76	7	287	8.7	0.22	6.5	3.1
651228	2 9	50.03	19	18.81	155	17.23	6.34	2.50	6	264	7.0	0.09	3.6	0.7
651228	224	21.52	19	18.91	155	13.88	5.73	1.90	7	226	7.3	0.08	1.2	0.8
651228	232	16.42	19	15.81	155	21.75	8.07	2.65	7	280	8.5	0.21	3.7	26.4
651228	245	21.75	19	20.28	155	18.90	5.00	2.83	7	216	6.6	0.24	5.5	9.1
651228	316	51.88	19	20.85	155	16.71	2.39	1.60	7	183	3.2	0.14	1.3	14.6
651228	328	26.27	19	22.77	155	20.36	6.65	2.57	4	187	6.1	0.00	0.0	0.0
651228	335	1.09	19	20.20	155	17.89	2.44	2.44	8	192	5.4	0.10	0.8	1.5
651228	336	50.83	19	22.35	155	14.68	1.31	3.25	7	176	2.1	0.17	4.0	2.4
651228	441	31.84	19	19.21	155	17.82	4.04	3.20	10	210	6.8	0.17	1.1	0.7
651228	459	15.82	19	20.27	155	17.92	4.36	3.16	13	146	5.3	0.17	0.8	0.6
651228	518	14.22	19	19.50	155	17.80	5.05	3.04	14	205	6.3	0.19	0.9	0.7
651228	7 0	24.29	19	21.61	155	15.64	5.00	1.77	9	171	1.5	0.12	0.8	0.7
651228	720	16.10	19	20.01	155	20.37	5.00	2.19	6	213	5.1	0.40	3.9	7.4
651228	731	49.10	19	19.92	155	18.86	5.20	2.84	11	196	6.9	0.22	1.4	0.7
651228	8 4	58.45	19	17.61	155	13.41	6.96	2.53	11	248	9.8	0.13	1.2	0.5
651228	8 9	12.19	19	22.50	155	16.93	1.99	0.89	5	250	1.8	0.18	14.5	1.5
651228	916	9.74	19	20.79	155	19.40	5.68	2.56	8	177	6.8	0.23	1.8	3.4
651228	929	16.00	19	19.46	155	13.91	5.05	1.68	6	217	6.4	0.05	0.7	1.8
651228	1029	50.45	19	22.50	155	16.00	0.70	3.22	12	115	0.3	0.74	2.7	0.7
651228	1059	52.86	19	19.72	155	17.88	5.71	3.12	7	201	6.0	0.06	0.6	1.5
651228	1118	1.82	19	21.00	155	16.00	5.00	3.83	9	181	2.6	0.25	1.8	1.2
651228	1127	53.41	19	10.62	155	19.61	4.30	2.73	9	301	18.8	0.13	1.7	1.0
651228	1134	58.22	19	19.70	155	17.32	7.41	3.20	12	202	5.6	0.13	0.8	0.4
651228	1230	10.89	19	21.98	155	16.28	6.95	2.86	9	163	1.0	0.13	0.9	0.5
651228	1359	40.38	19	18.99	155	15.24	7.34	1.34	7	218	6.4	0.04	0.5	0.3
651228	15 5	33.98	19	25.54	155	19.48	35.83	2.36	4	251	4.5	0.04	0.0	0.0
651228	1513	59.33	19	11.89	155	16.01	3.00	1.71	3	353	19.4	0.04	0.0	0.0
651228	1516	23.98	19	17.01	155	20.38	5.00	2.32	7	255	7.8	0.33	4.2	8.9
651228	1522	44.37	19	14.76	155	20.63	10.36	2.83	6	280	11.1	0.02	0.4	0.7
651228	1528	21.16	19	20.07	155	17.62	3.10	2.53	7	236	5.3	0.12	2.1	5.4
651228	1548	48.79	19	19.53	155	14.70	4.67	2.61	4	343	5.7	0.01	0.0	0.0
651228	1618	15.85	19	17.79	155	20.70	4.00	3.69	13	224	6.4	0.28	2.0	1.1
651228	1646	20.64	19	12.36	155	16.01	3.00	1.93	3	353	18.5	0.08	0.0	0.0
651228	1650	37.52	19	22.37	155	16.45	0.41	0.11	4	250	1.0	0.14	0.0	0.0
651228	17 4	47.70	19	17.40	155	15.43	7.08	1.82	6	296	9.3	0.14	5.1	4.6
651228	1745	44.82	19	19.61	155	18.17	6.02	2.99	8	260	6.5	0.12	2.8	0.8
651228	1826	42.59	19	19.49	155	17.68	2.17	2.52	6	247	6.2	0.21	4.8	2.1
651228	1843	15.99	19	22.50	155	15.51	2.13	1.23	10	155	0.7	0.27	2.0	0.7
651228	1849	14.20	19	24.25	155	16.83	0.55	1.27	6	169	1.2	0.18	1.2	0.5
651228	1856	0.81	19	16.70	155	16.01	3.00	0.31	3	296	10.5	0.17	0.0	0.0
651228	1935	25.26	19	20.50	155	17.00	2.62	0.44	4	238	4.0	0.17	0.0	0.0
651228	1947	1.04	19	19.77	155	15.43	0.98	1.23	4	283	4.9	0.11	0.0	0.0
651228	2023	29.55	19	12.42	155	12.98	5.47	1.70	5	292	18.1	0.09	1.1	0.4
651228	2040	6.20	19	20.41	155	17.97	5.00	2.17	4	223	5.2	0.12	0.0	0.0
651228	2051	27.36	19	20.05	155	17.79	5.63	3.42	9	195	5.5	0.24	1.8	1.3
651228	2113	41.38	19	19.79	155	18.22	2.00	1.23	7	235	6.3	0.20	2.5	2.2
651228	2114	19.11	19	22.50	155	16.00	9.11	1.23	6	119	0.3	0.25	3.5	3.3
651228	2115	7.17	19	22.50	155	16.00	1.96	2.69	4	158	0.3	0.26	0.0	0.0

651228	2127	17.40	19	22.10	155	16.78	0.91	1.95	4	275	1.6	0.01	0.0	0.0
651228	2141	41.55	19	22.41	155	15.76	7.00	2.78	6	156	0.2	0.24	2.9	4.2
651228	2210	54.38	19	20.30	155	18.93	3.27	2.32	6	215	6.6	0.19	7.2	44.5
651228	2222	8.15	19	23.61	155	11.08	4.00	2.81	11	135	3.8	0.12	0.8	0.7
651228	2239	27.45	19	20.13	155	16.76	1.85	3.50	7	245	4.5	0.13	2.7	1.1
651228	2253	27.21	19	21.96	155	15.43	7.36	1.61	6	284	1.2	0.17	3.0	1.9
651228	2312	31.36	19	20.57	155	16.57	0.00	2.48	6	248	3.6	0.12	3.3	3.5
651228	2319	4.94	19	18.31	155	16.25	6.02	3.13	7	281	7.6	0.10	1.6	0.7
651229	016	32.46	19	23.22	155	24.48	5.76	2.27	7	210	5.9	0.15	1.4	1.1
651229	020	26.01	19	19.84	155	17.71	9.85	0.88	6	199	5.7	0.02	0.4	0.8
651229	021	33.88	19	23.04	155	15.43	8.05	1.92	4	254	1.4	0.05	0.0	0.0
651229	1 7	18.43	19	12.37	155	17.80	5.00	2.15	4	316	17.4	0.12	0.0	0.0
651229	1 9	13.25	19	19.92	155	17.17	5.41	2.44	10	198	9.2	0.18	1.1	1.0
651229	128	12.73	19	23.04	155	15.43	6.00	1.97	11	142	1.4	0.23	1.5	1.4
651229	220	5.98	19	9.61	155	11.65	2.27	2.75	3	357	24.7	0.10	0.0	0.0
651229	224	44.68	19	20.66	155	18.77	5.00	2.44	5	206	6.0	0.05	2.2	6.9
651229	226	55.46	19	18.50	155	13.38	8.08	1.50	8	236	8.4	0.18	3.0	17.1
651229	245	13.65	19	20.06	155	17.83	4.07	2.91	6	234	5.5	0.06	0.6	1.8
651229	334	15.26	19	21.67	155	18.99	5.00	2.79	5	161	6.2	0.29	10.6	40.6
651229	341	14.64	19	16.42	155	19.97	4.27	1.43	10	233	9.1	0.25	1.9	1.7
651229	343	20.71	19	13.24	155	16.85	3.56	2.40	6	281	17.0	0.14	5.1	2.0
651229	343	44.28	19	21.77	155	15.43	4.00	3.46	11	168	1.4	0.25	1.3	0.9
651229	352	37.05	19	16.66	155	18.28	3.87	2.04	7	250	11.0	0.22	1.8	13.1
651229	430	19.42	19	20.70	155	16.62	2.84	3.40	8	185	7.5	0.19	1.4	1.3
651229	435	22.54	19	20.75	155	16.38	0.26	1.94	6	185	3.2	0.07	0.7	2.5
651229	444	26.98	19	25.00	155	4.33	5.00	1.27	3	357	22.2	0.05	0.0	0.0
651229	456	17.85	19	19.97	155	18.36	5.00	2.81	6	229	6.2	0.10	5.2	12.5
651229	555	50.92	19	19.87	155	17.40	6.97	2.63	7	199	5.4	0.05	0.6	0.4
651229	6 2	3.16	19	19.77	155	17.95	3.27	1.96	4	238	6.0	0.17	0.0	0.0
651229	6 5	11.82	19	20.52	155	18.49	0.54	2.78	4	213	5.7	0.15	0.0	0.0
651229	6 6	9.91	19	22.35	155	8.72	16.11	1.98	7	237	2.5	0.14	3.3	2.0
651229	6 9	44.05	19	22.50	155	16.73	5.00	2.21	4	153	1.5	0.08	0.0	0.0
651229	659	3.75	19	21.08	155	17.10	6.19	3.09	6	178	6.7	0.23	2.4	6.3
651229	712	12.05	19	21.34	155	17.24	5.00	3.09	8	173	3.1	0.16	1.1	1.2
651229	734	53.34	19	11.36	155	10.80	3.27	3.24	7	303	19.3	0.12	7.1	2.4
651229	748	1.39	19	17.40	155	17.34	6.97	2.94	10	239	9.6	0.17	1.9	0.7
651229	752	28.18	19	19.53	155	16.46	5.49	3.25	9	206	5.4	0.18	1.6	0.8
651229	825	24.58	19	19.63	155	17.80	3.39	2.56	8	203	6.1	0.14	1.2	4.5
651229	834	31.55	19	20.25	155	18.55	5.00	2.82	6	190	6.1	0.23	2.4	6.6
651229	858	6.64	19	19.42	155	18.20	4.58	3.79	7	206	6.8	0.11	1.2	1.1
651229	911	36.44	19	20.30	155	19.50	0.00	2.34	6	188	6.7	0.26	3.1	15.8
651229	930	33.45	19	15.36	155	11.95	6.32	2.52	7	278	12.4	0.10	2.7	0.9
651229	937	43.94	19	21.25	155	16.00	3.84	1.69	4	253	2.1	0.06	0.0	0.0
651229	10 5	47.26	19	20.73	155	15.52	1.03	1.74	5	280	2.1	0.09	0.1	0.1
651229	10 6	45.98	19	21.18	155	16.80	1.13	3.06	8	92	0.9	0.09	0.5	0.3
651229	1040	16.98	19	15.99	155	16.71	6.37	2.01	6	297	11.9	0.11	3.7	1.0
651229	12 7	22.87	19	18.64	155	16.27	6.00	1.83	5	278	7.0	0.17	8.6	6.2
651229	1227	12.10	19	20.32	155	17.77	3.27	2.62	8	161	5.0	0.08	0.6	4.2
651229	1246	9.55	19	20.33	155	17.77	5.57	3.28	9	161	5.0	0.09	0.5	1.4
651229	1249	33.26	19	19.63	155	18.09	5.93	2.57	6	179	6.4	0.18	1.8	6.9

651229	13 6	51.13	19	20.60	155	16.02	1.38	1.78	7	144	3.3	0.09	0.6	0.5
651229	1329	27.85	19	20.38	155	18.27	5.06	2.84	11	161	5.6	0.07	0.4	0.9
651229	1517	48.57	19	20.78	155	17.14	5.42	3.80	11	183	3.7	0.15	0.9	0.6
651229	1731	19.40	19	21.42	155	15.52	1.27	2.94	8	175	1.9	0.18	1.3	1.1
651229	21 4	50.09	19	20.05	155	17.72	4.14	2.15	7	235	5.4	0.04	0.9	1.4
651229	2114	59.98	19	20.96	155	17.10	5.72	2.83	7	180	6.9	0.12	1.1	1.1
651229	2122	30.13	19	21.52	155	17.33	2.07	1.56	6	200	3.0	0.10	0.6	1.0
651229	2213	20.83	19	11.32	155	18.43	9.39	2.46	8	262	18.5	0.14	5.3	3.9
651229	2232	42.53	19	18.38	155	15.43	2.27	3.06	4	290	7.5	0.21	0.0	0.0
651230	010	55.63	19	21.30	155	16.00	5.59	4.27	12	176	2.0	0.15	0.8	0.5
651230	017	11.68	19	20.85	155	16.00	0.22	2.42	8	184	2.9	0.12	0.6	0.5
651230	047	46.22	19	20.04	155	16.98	6.71	3.00	7	196	8.6	0.13	1.2	0.9
651230	053	42.77	19	20.39	155	16.52	5.00	3.28	7	191	3.9	0.09	0.8	1.8
651230	148	27.05	19	20.28	155	9.23	7.43	2.36	5	295	3.1	0.08	2.8	0.6
651230	157	19.64	19	20.90	155	16.85	0.29	1.89	6	181	3.2	0.04	0.1	0.3
651230	214	24.37	19	21.86	155	16.37	5.00	2.17	10	165	1.3	0.16	0.9	0.7
651230	215	12.35	19	21.09	155	16.00	1.94	1.23	4	259	2.4	0.01	0.0	0.0
651230	3 3	30.34	19	21.56	155	11.92	7.14	3.06	11	200	3.4	0.22	1.5	0.7
651230	514	46.26	19	13.87	155	10.55	9.04	2.24	6	327	18.3	0.10	4.8	27.4
651230	550	58.25	19	20.40	155	16.00	2.61	1.73	6	265	3.7	0.15	3.0	11.3
651230	639	16.38	19	21.50	155	15.03	2.14	2.33	7	174	2.3	0.15	1.4	26.9
651230	652	50.08	19	18.25	155	13.14	7.97	1.60	7	241	8.6	0.09	8.4	5.2

APPENDIX B

SEISMOGRAPH LOCATIONS

The following locations of both fixed and portable seismographs during late December, 1965 earthquake swarm are displayed;

FIXED STATIONS

STATION	LATITUDE	LONGITUDE	ELEVATION	DELAY
MLO	19-29.80N	155-23.30W	2010	+0.03
AHU	19-22.40N	155-15.90W	1070	-0.10
AHE	19-22.40N	155-15.90W	1070	-0.10
AHN	19-22.40N	155-15.90W	1070	-0.10
DES	19-20.20N	155-23.30W	815	-0.29
NPT	19-24.90N	155-17.00W	1115	-0.30
WPT	19-24.70N	155-17.50W	1115	-0.26
MPH	19-21.80N	155-10.00W	885	-0.17
UWE	19-25.40N	155-17.60W	1240	-0.21
USE	19-25.40N	155-17.60W	1240	-0.21
USZ	19-25.40N	155-17.60W	1240	-0.21
PHA	19-29.70N	154-56.80W	205	-0.17
NAL	19-03.80N	155-35.20W	205	+0.03
HIL	19-43.20N	155-05.30W	20	+0.54
HIE	19-43.20N	155-05.30W	20	+0.54
HIN	19-43.20N	155-05.30W	20	+0.54
KLK	19-31.20N	155-55.30W	505	0.00

KLN	19-31.20N	155-55.30W	505	0.00
KLE	19-31.20N	155-55.30W	505	0.00
NBY	19-29.70N	155-34.80W	4005	+0.09

PORTABLE STATIONS

PSS1	19-20.70N	155-16.70W	3180	0.00
PSS2	19-22.90N	155-14.50W	3400	0.00
PSS3	19-24.50N	155-20.20W	3564	0.00
PSS4	19-21.70N	155-13.70W	3200	0.00
PSS5	19-19.00N	155-13.40W	2000	0.00

APPENDIX C

CLOCK CORRECTIONS

All seismographs in operation during the December, 1965, earthquake swarm were standardized to a common WWVH time signal. The WWVH signal was recorded twice a day on each seismogram. Minute and hour marks (15 minutes to a line, 4 lines for every hour) were recorded on the seismograms using individual clocks internal to each station. Drift of these internal clocks could be determined by measuring the difference in offset between the WWVH clock minute and the appropriate internal clock minute at the beginning and end of each seismogram. Drift was assumed to be linear and could be incorporated into each arrival time reading, to insure a common time source for each earthquake location.

Stations USZ, WPT, NPT, MPH, MLO, DES, and AHU, located near the summit of Kilauea (Appendix B, Fig. 2), were all hard wired to a common clock located at station USZ. Stations PHA, NBY, NAL, KLK, and HIL, at a distance from the Kilauea summit (Appendix B, Fig. 1), were each wired to individual clocks. It was determined that an offset occurred in USZ clock sometime between 0700, December 24, and 1000, December 26 (Fig. 14). WWVH could not be read during this time, due to the masking effect of the high levels of earthquakes and tremor. In order to locate earthquakes between 1300, December 25, and 1000, December 26, a clock correction was needed for the USZ clock.

USZ clock corrections were calculated by interpolating between the readings made at 0700, December 24, and 1000, December 26. When earthquake locations were attempted for the time period 1300, December 25, to 1000, December 26, using both near (USZ clock) and far Kilauea stations, poor time residuals (in excess of 0.5 seconds) were obtained. Using either the far Kilauea stations alone, or the near (USZ clock) Kilauea stations alone, good time residuals on the order of 0.1 seconds were obtained. This suggests that all far Kilauea stations had fairly accurate clock corrections, and that the near Kilauea (USZ clock) clock corrections were in error. In order to rectify this situation, several well located earthquakes from this time period were chosen to determine a good clock correction for the inner stations. Near-Kilauea station arrivals were used for locating the earthquakes. Of primary interest was the location of each earthquake, so even though the USZ clock correction was faulty, all inner stations tied into a common time source would still provide a reliable location. These locations had time residuals on the order of 0.1 seconds. Assuming these locations correct, the time residuals from the far Kilauea stations were calculated. These residuals, determined from the inner station earthquake location and origin time, are thus analogus to the offset in the USZ clock. The offset is inherent in the computed origin time, using only the inner station arrival times to locate an earthquake. The residuals from these outer stations did not have a random distribution, rather they had values in close agreement with each other, which would be expected for an offset in the USZ clock. A linear fit to the mean of these residuals was made (Fig. 15). From this fit a correction (the difference between the fit and the old USZ clock correction for a given time) could be made to the USZ times.

When corrected values were applied to the USZ times, previous poorly located earthquakes, using both inner and outer stations, displayed much smaller time residuals. When the corrected USZ clock values were plotted for this time period (Fig. 14), they fall on an extension of the USZ clock correction line plotted for the December 25, 1000 and subsequent data points. No offset in this short extension exists, so it must be assumed that the USZ offset occurred sometime between 0700, December 24, and 1600, December 25. Unfortunately, not being able to locate these earthquakes due to the high activity levels, the time of offset cannot be determined. An explaination for the offset (R. Koyanagi, personal comm., 1980) is that strong ground movement might have jolted the pendulum clock at the USZ station. This station was close to the site of faulting and cracking.

An offset is also observable for station KLK (Fig. 14). Due to KLK's far distance from the activity (Fig. 1), only large earthquake arrivals could be read, and these were infrequent. For this reason the exact time of offset could not be determined. Extrapolations of the lower and upper clock corrections were used, dependent upon insuring good time residuals and continuity in earthquake solutions.

APPENDIX D

TRIAL FOCAL DEPTH STUDY

HYPO71 requires a trial focal depth for each earthquake location (Lee and Lahr, 1975). Local origin and small S-P time differences dictate a shallow trial depth for the late December, 1965, seismicity. A test, locating 64 events from the complete data set with trial depths of 0.01, 5.00, 10.00, and 25.00 kilometers, was performed in order to choose an appropriate trial depth.

The set of events having the smallest time residuals (RMS) had a trial focal depth of 5.00 kilometers (Table 1A). However, test runs using 0.10 and 10.00 kilometers as trial depths also had a large number of earthquakes with low RMS values (Table 1A). The set of events located with a 25.00 kilometer trial depth had poor residuals compared to the other sets, and was discarded as a choice for a trial depth (Table 1A).

To further constrain the choice for a trial focal depth, a comparison of trial depth to the final focal depth was made for each earthquake. HYPO71 can treat each variable in the adjustment vector (origin time, depth, latitude, and longitude) independently in the step-wise multiple regression procedure used in locating the earthquake (Lee and Lahr, 1975). A statistical analysis is performed to determine which variable is to be included in the regression (Lee and Lahr, 1975). A variable not included in the regression remains the same, and it's associated coordinate in time or space is fixed for the final solution.

There are times when a final coordinate is the same as it's trial coordinate. This can sometimes produce a computational artifact, such as lineations at certain depths, along particular latitudes, etc. The coordinates that comprise these lineations are in fact very close to what they should be. The program determined that these trial values needed no further adjustments and fixed them as is. Bearing this in mind, the best candidate for a trial focal depth is one that has the greatest number of earthquakes located with depths equivalent to their trial depths. A trial depth of 5.00 kilometers was found to fit this criteria well (Table 1B), and was therefore used for the entire data set. For earthquakes having poor residuals, or hypocenters which did not converge to a minimum RMS value, trial coordinates were adjusted until a good solution was obtained. The method used to determine new trial coordinates is similar to the RMS map contouring procedure described earlier in the text.

Table 1. Focal depths used in trial focal depth study. Table 1A; lists % of events having RMS less than 0.30 seconds, Table 1B; lists the number of final focal depths equivalent to the trial focal depth.

A.

TRIAL FOCAL DEPTH	%* EVENTS HAVING RMS 0.30 SECONDS
05.00 km	81 %
10.00 km	78 %
00.10 km	73 %
25.00 km	53 %

B.

TRIAL FOCAL DEPTH	%* EVENTS (TRIAL DEPTH=FOCAL DEPTH)
05.00 km	34 %
10.00 km	14 %
00.10 km	19 %
25.00 km	17 %

* out of a set of 64 earthquakes

Fig. 1. Map of the island of Hawaii. Solid triangles are the locations of fixed seismograph instruments outside the Kilauea vicinity in operation during the late December, 1965, earthquake swarm. Solid circles are the locations of the summits of Hawaii volcanoes.

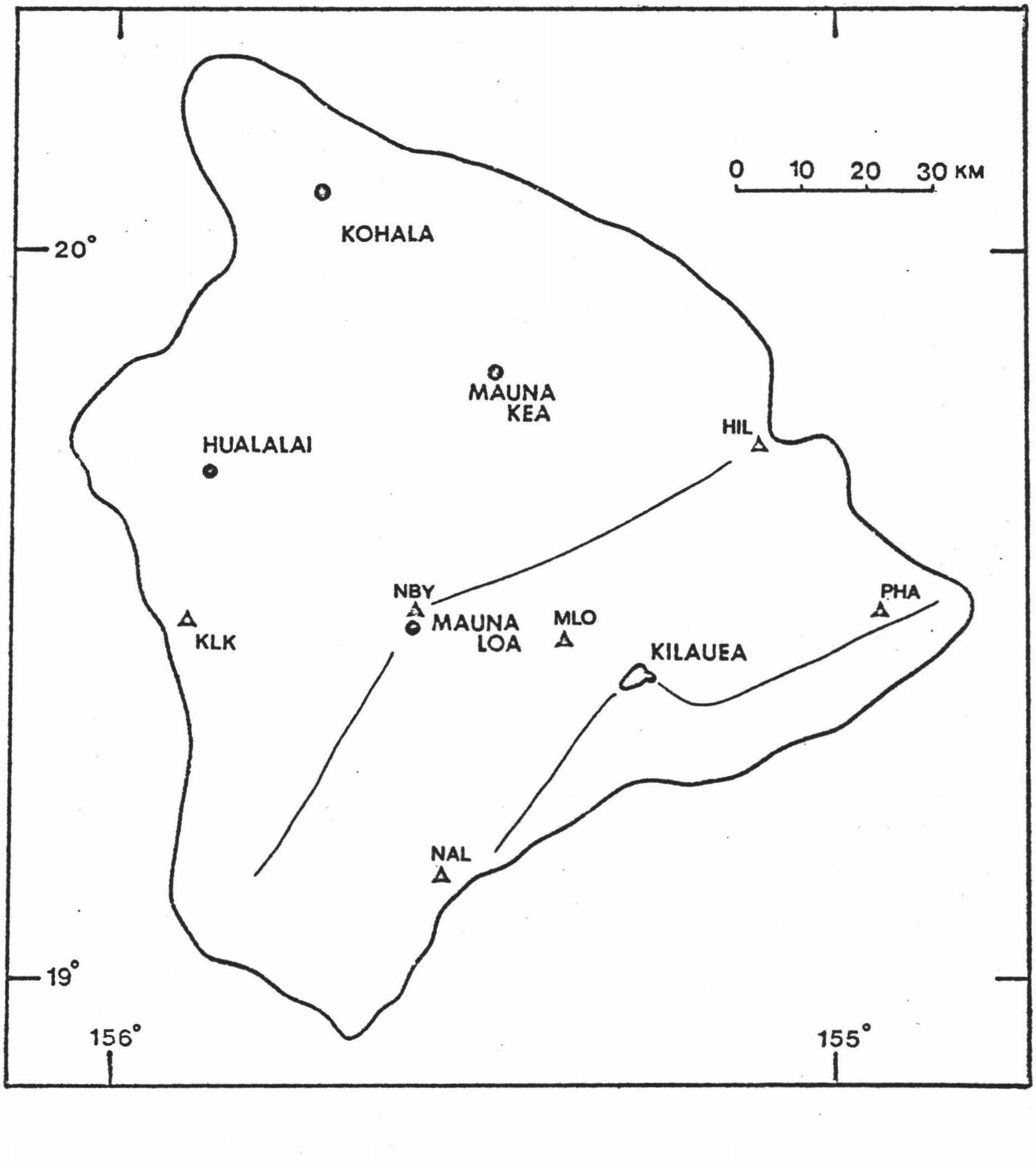

0 10 20 30 KM
KOHALA
20°
MAUNA
KEA
HIL
HUALALAI
NBY
MAUNA
LOA
MLO
PHA
KLK
KILAUEA
NAL
19°
156°
155°

Fig. 2. Map of Kilauea Volcano. Structural features, roads, and seismic stations are displayed (Fiske and Koyanagi, 1968).

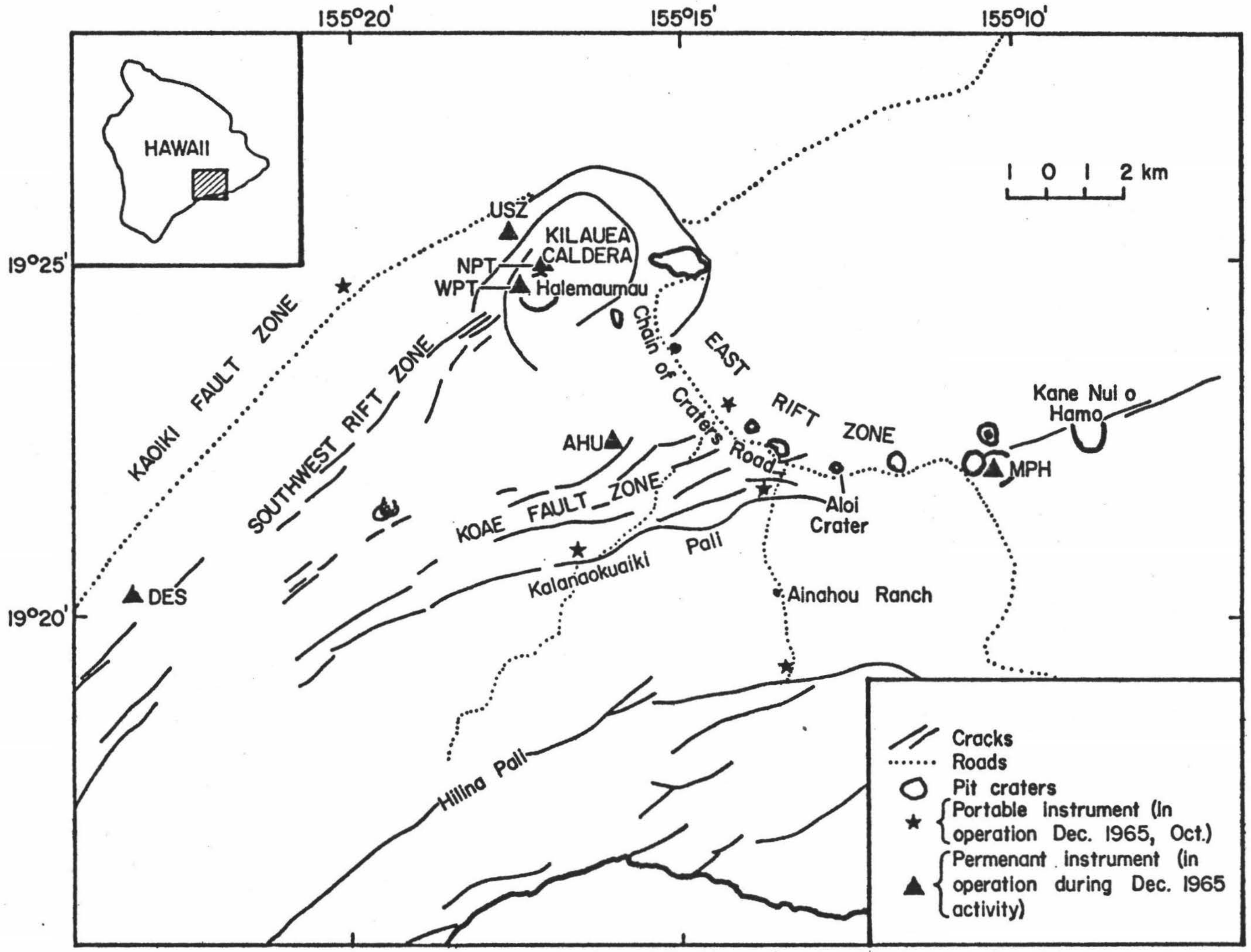
155°20'
155°15'
155°10'
19°25'
19°20'
HAWAII
1 0 1 2 km
USZ
KILAUEA CALDERA
NPT
WPT
Halemaumau
KAOIKI FAULT ZONE
SOUTHWEST RIFT ZONE
Chain of Craters Road
EAST RIFT ZONE
Kane Nui o Hamo
MPH
AHU
KOAE FAULT ZONE
Aloi Crater
Kalanaokuaiki Pali
Ainahou Ranch
DES
Hilina Pali
Cracks
Roads
Pit craters
Portable instrument (in operation Dec. 1965, Oct.)
Permenant instrument (in operation during Dec. 1965 activity)

Fig. 3. Chronology of the events associated with the December, 1965, eruption of Kilauea. The duration of the eruption has been projected downward (dotted lines) to emphasize that the eruption occupied only the early stage of the total activity (Fiske and Koyanagi, 1965).

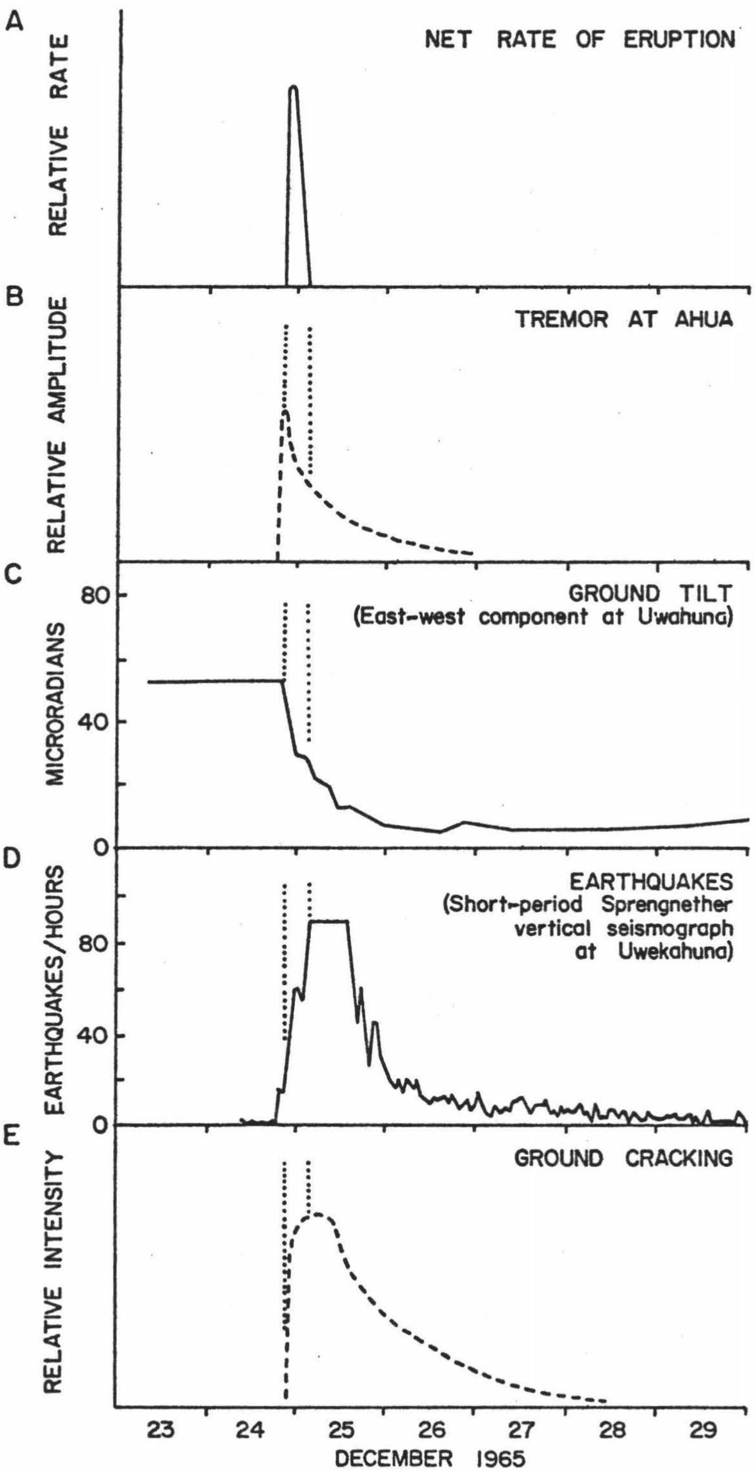
A
RELATIVE RATE
NET RATE OF ERUPTION
B
RELATIVE AMPLITUDE
TREMOR AT AHUA
C
MICRORADIANS
80
40
0
GROUND TILT
(East-west component at Uwahuna)
D
EARTHQUAKES/HOURS
80
40
0
EARTHQUAKES
(Short-period Sprengnether
vertical seismograph
at Uwekahuna)
E
RELATIVE INTENSITY
GROUND CRACKING
23
24
25
26
27
28
29
DECEMBER 1965

Fig. 4. Seismograms read for the December, 1965, earthquake swarm. From top to bottom the records are optical, pen, smoked paper, and strip chart.

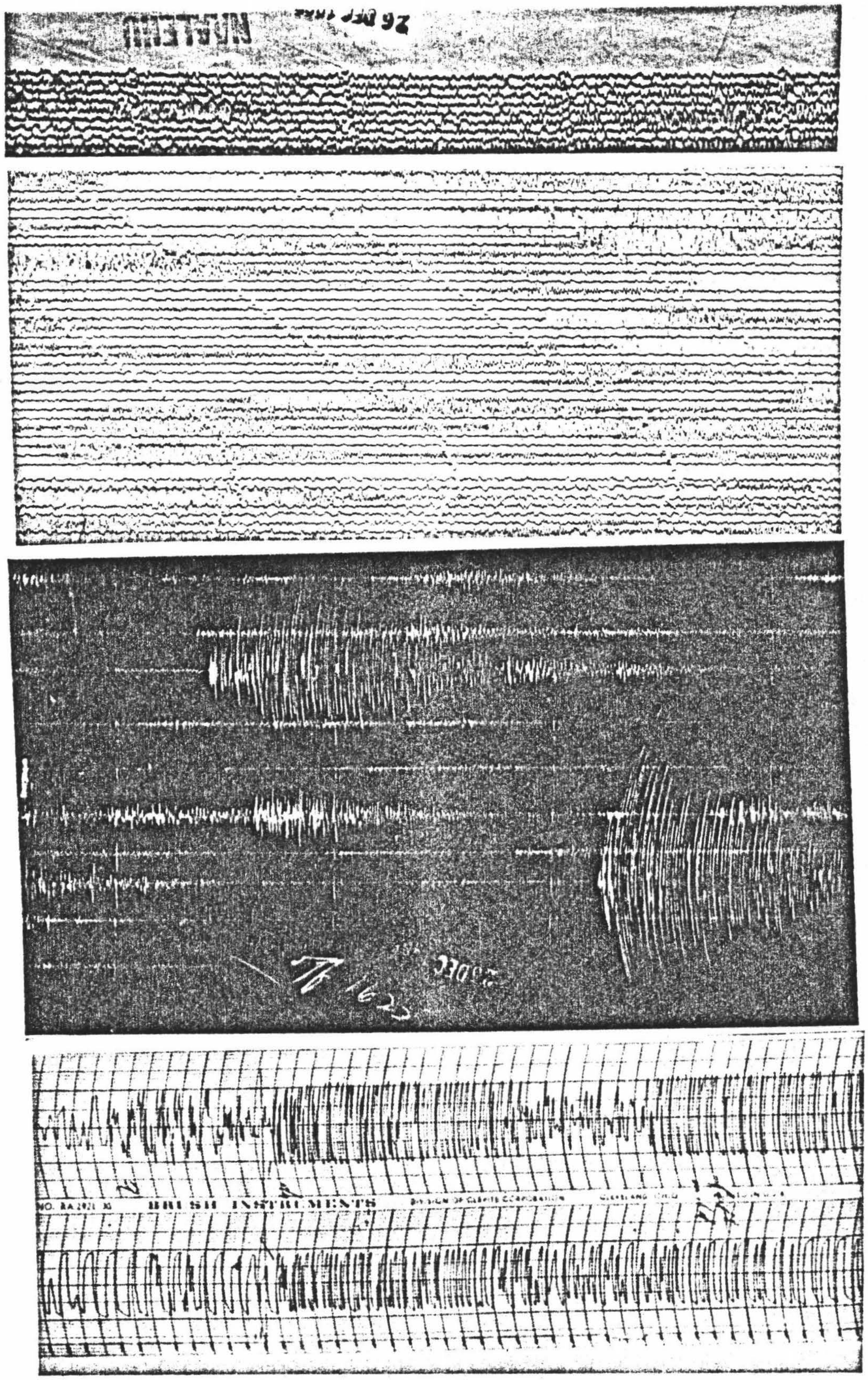
BRUSH INSTRUMENTS

Fig. 5. Contour map of RMS time residuals for an earthquake located at 19-21.18N, 155-16.80W, at a depth of 1.13 kilometers. Forced solutions have been plotted 1 km apart both in the horizontal (upper diagram) and the vertical plane (lower diagram) and their respective RMS time residuals were then contoured. The solid circle is the determined hypocenter. The solid triangles are the seismic stations used to locate the hypocenter, and forced solutions.

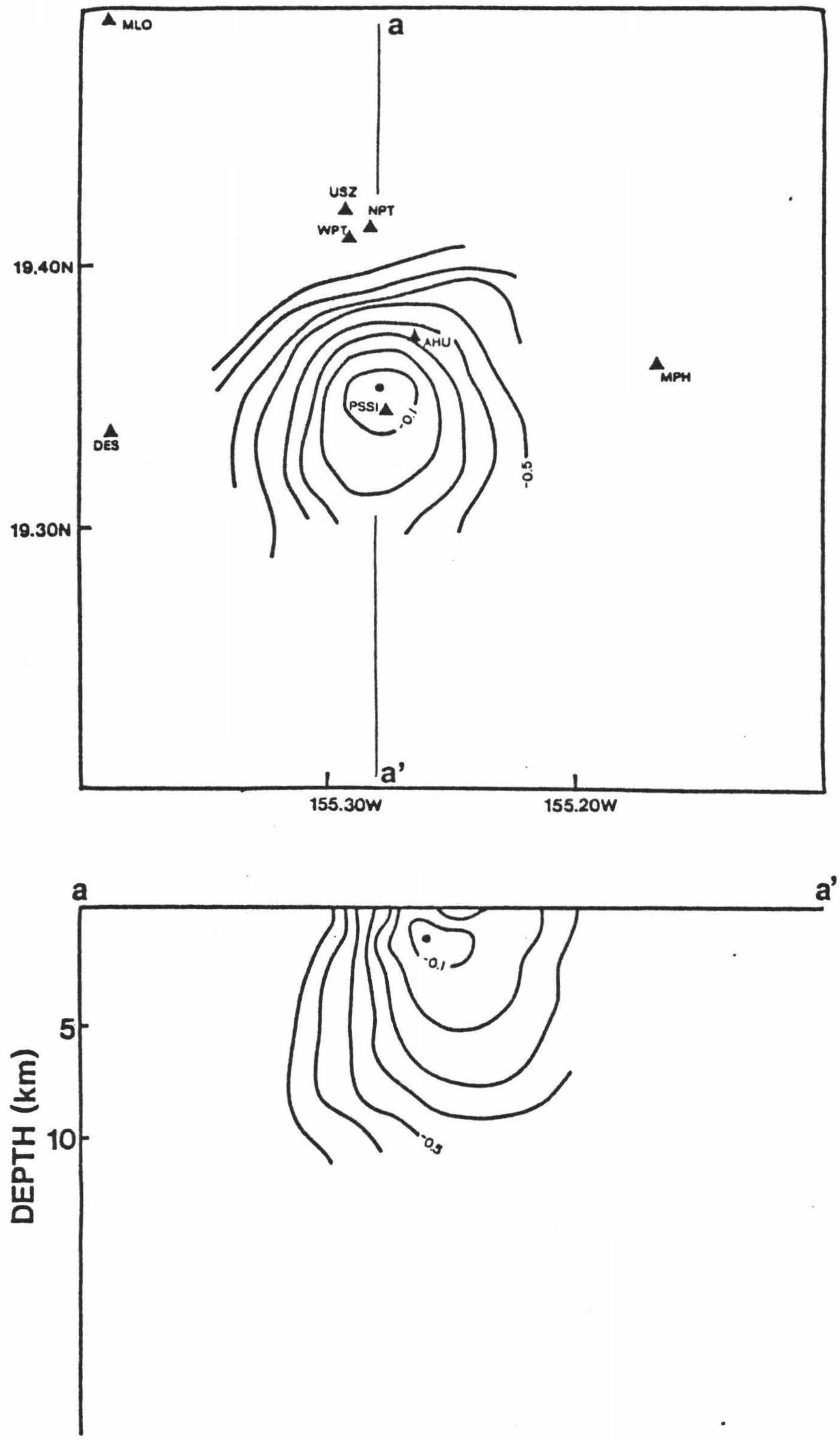
MLO
a
USZ
NPT
WPT
19.40N
AHU
MPH
PSSI
-0.1
DES
-0.5
19.30N
a'
155.30W
155.20W
a
a'
-0.1
5
DEPTH (km)
10
-0.5

Fig. 6. Contour map of RMS time residuals for an earthquake located at 19-11.55N, 155-13.17W, at a depth of 5.09 km. Forced solutions have been plotted 1 km apart both in the horizontal (upper diagram) and vertical plane (lower diagram) and their respective RMS time residuals were then contoured. Symbols and distance scale are the same as Fig. 5.

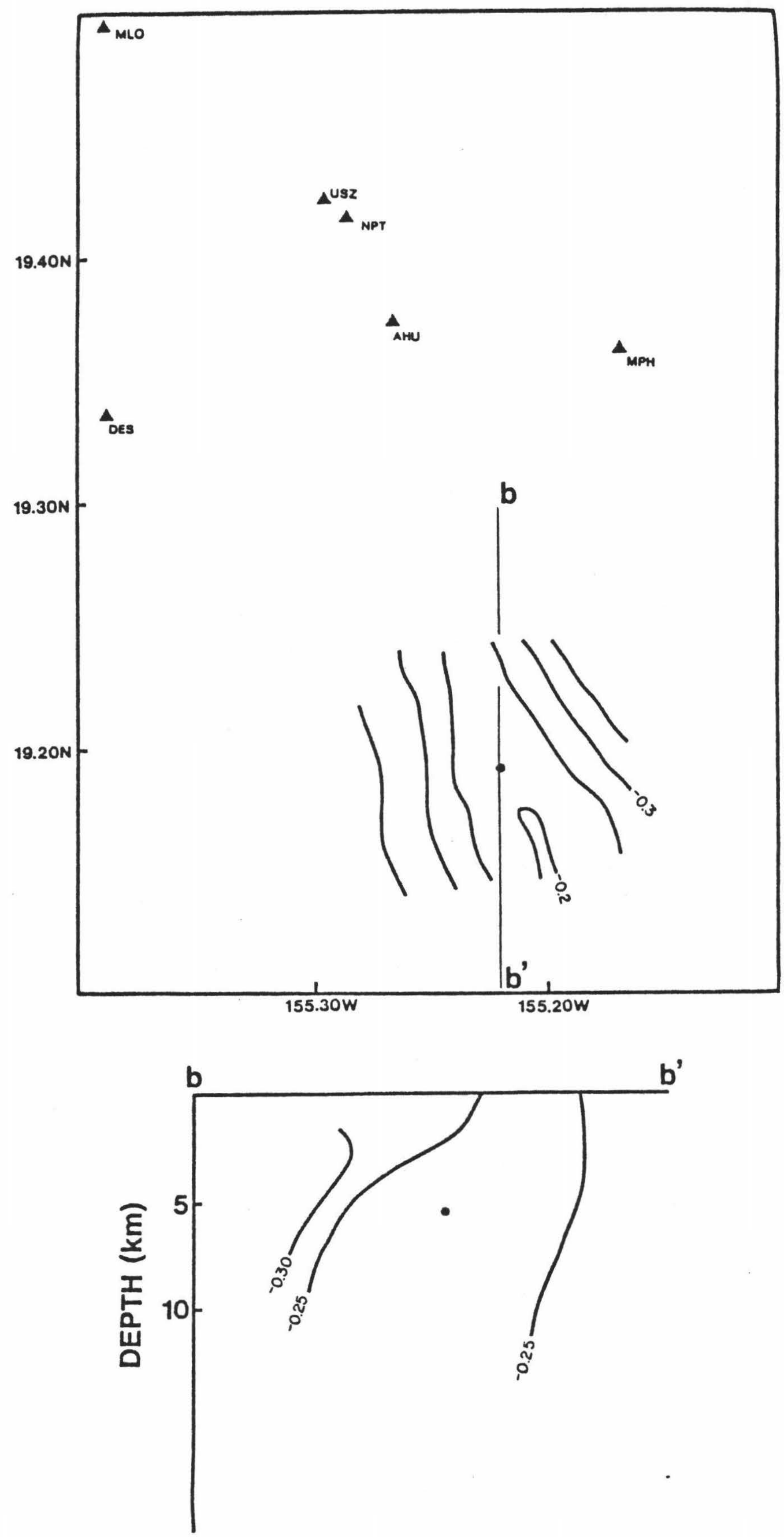
MLO
USZ
NPT
19.40N
AHU
MPH
DES
19.30N
b
19.20N
-0.3
-0.2
b'
155.30W
155.20W
b
b'
5
10
DEPTH (km)
-0.30
-0.25
-0.25

Fig. 7. Epicenter plot of all earthquakes located between 13:00, December, 25, to 08:00, December, 30 having RMS time residuals less than 0.3 seconds, horizontal and vertical standard errors less than 1.5 km, and using 5 or more stations for each location. Shaded area outlines a broad NE-SW trending ellipsoid of earthquakes in the Koae fault zone. Open circles are the epicenters, solid triangles are the location of fixed seismographs, solid squares are the location of the portable seismograph, and dotted lines are the location of the eruption at Aloi crater.

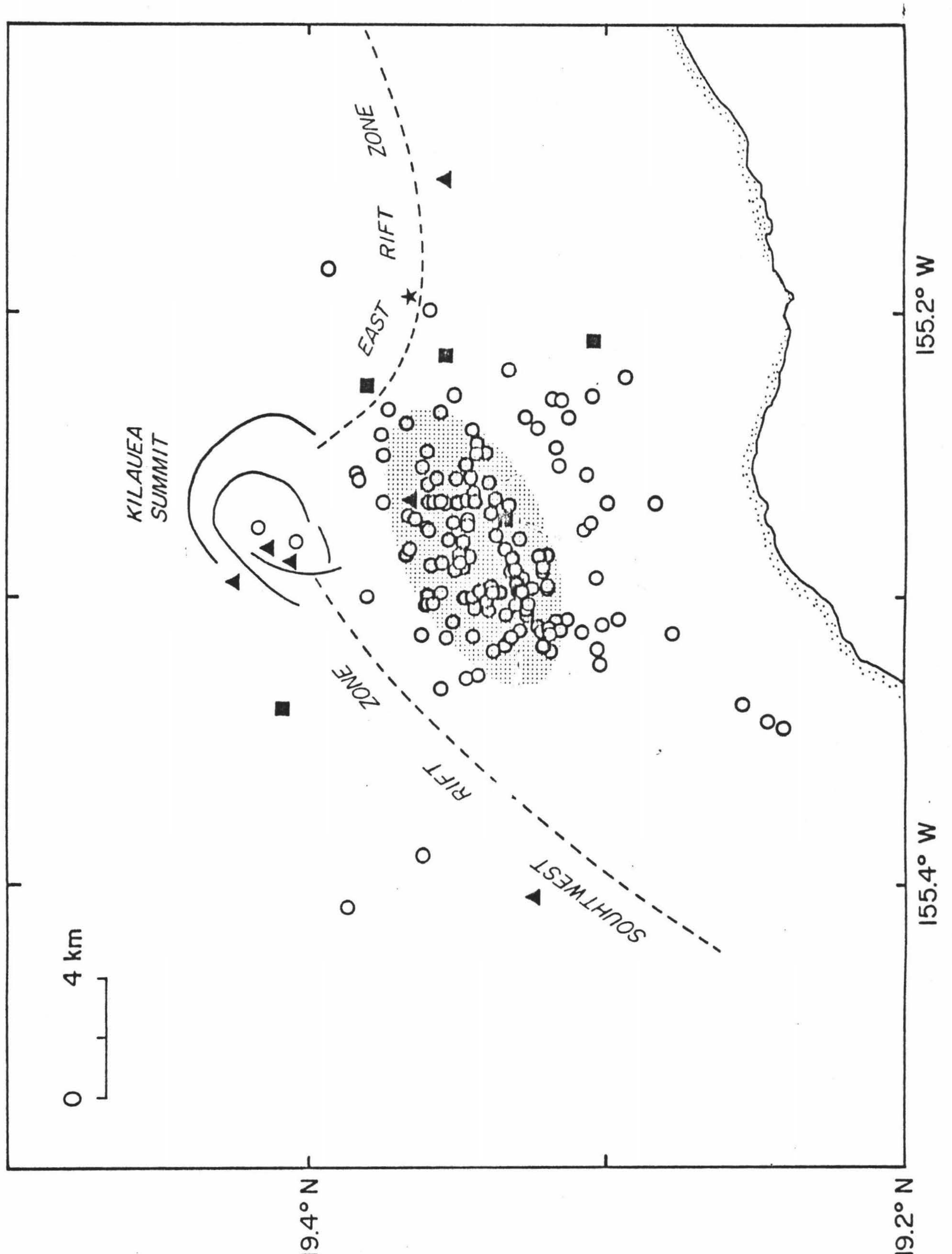
KILAUEA SUMMIT
EAST RIFT ZONE
SOUHTWEST RIFT ZONE
0 4 km
19.4° N
19.2° N
155.2° W
155.4° W

Fig. 8. Cross section parallel to the Koae fault zone. Open circles are hypocenters.

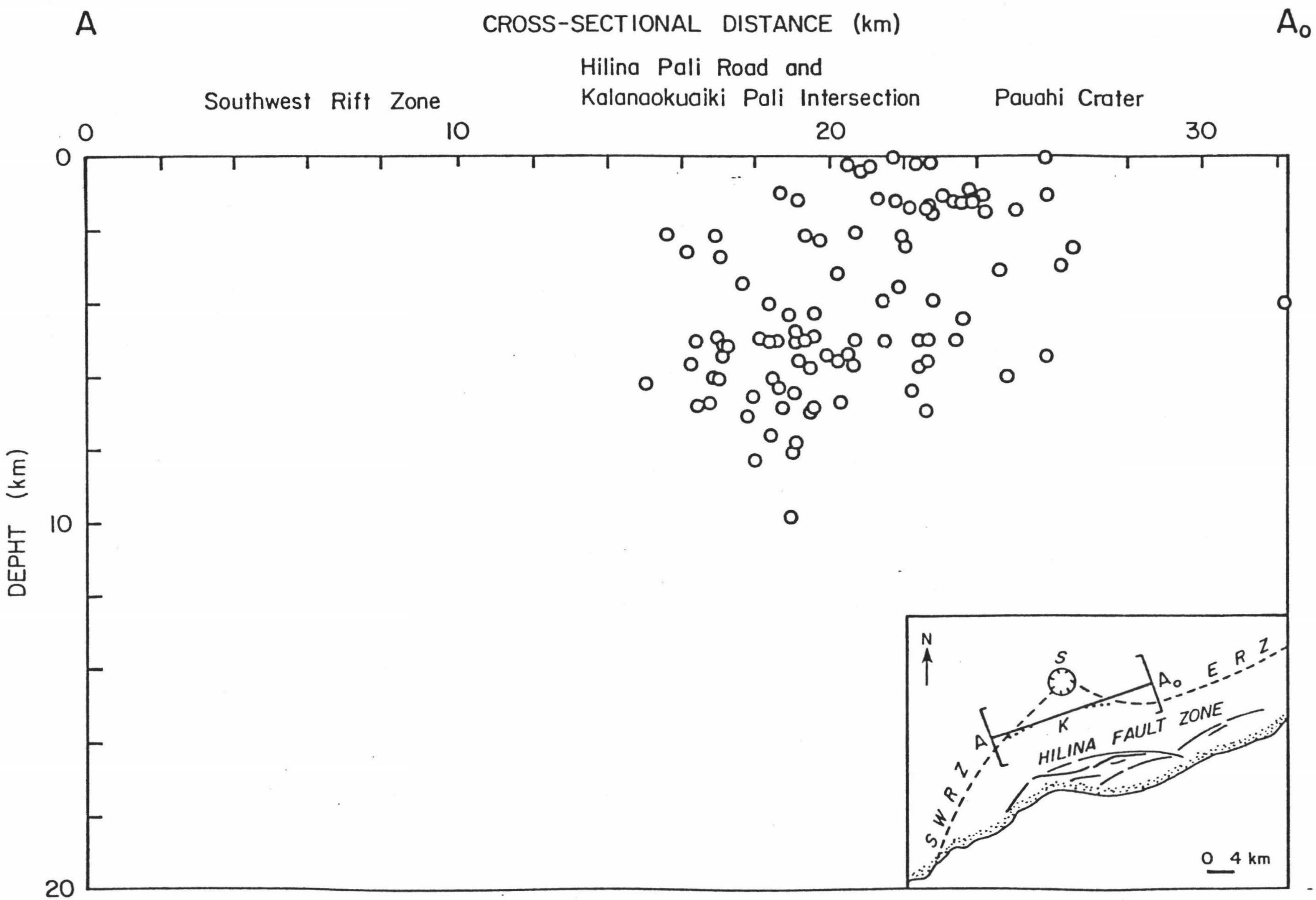
A
CROSS-SECTIONAL DISTANCE (km)
A$_o$
Hilina Pali Road and
Kalanaokuaiki Pali Intersection
Southwest Rift Zone
Pauahi Crater
0
10
20
30
0
10
20
DEPHT (km)
N
S
A$_o$
E R Z
K
HILINA FAULT ZONE
A
S W R Z
0 4 km

Fig. 9. Contoured earthquake density cross section of earthquakes per volume (cubic km) parallel to the Koae fault zone.

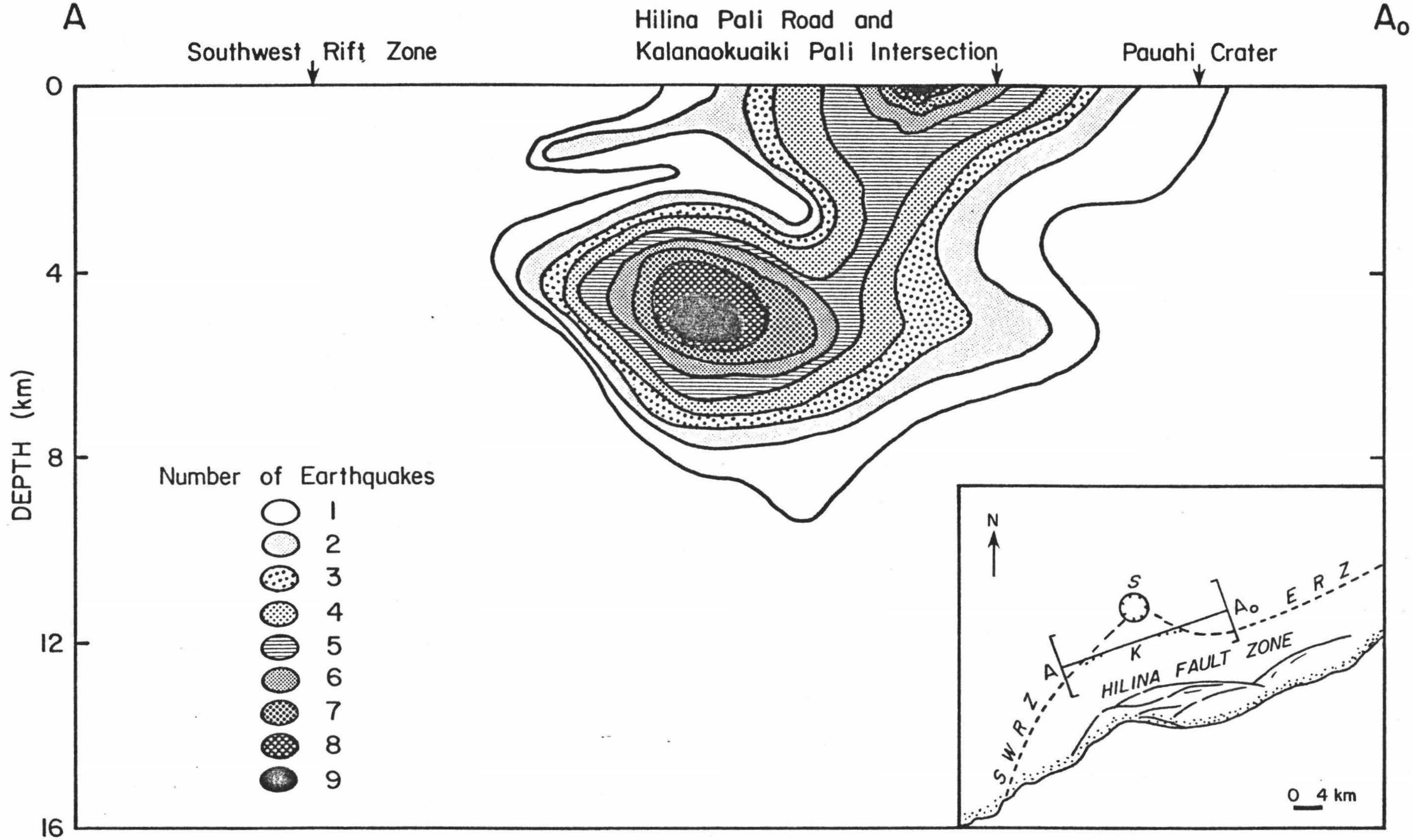

A
A₀
Southwest Rift Zone
Hilina Pali Road and
Kalanaokuaiki Pali Intersection
Pauahi Crater
0
4
8
12
16
DEPTH (km)
Number of Earthquakes
1
2
3
4
5
6
7
8
9
N
S
A₀
E R Z
K
A
HILINA FAULT ZONE
S W R Z
0 4 km

Fig. 10. Contoured earthquake density cross section of earthquakes per volume (cubic km) normal to the Koae fault zone. Section C-Co through the eastern Koae, and section D-Do through the central and western Koae.

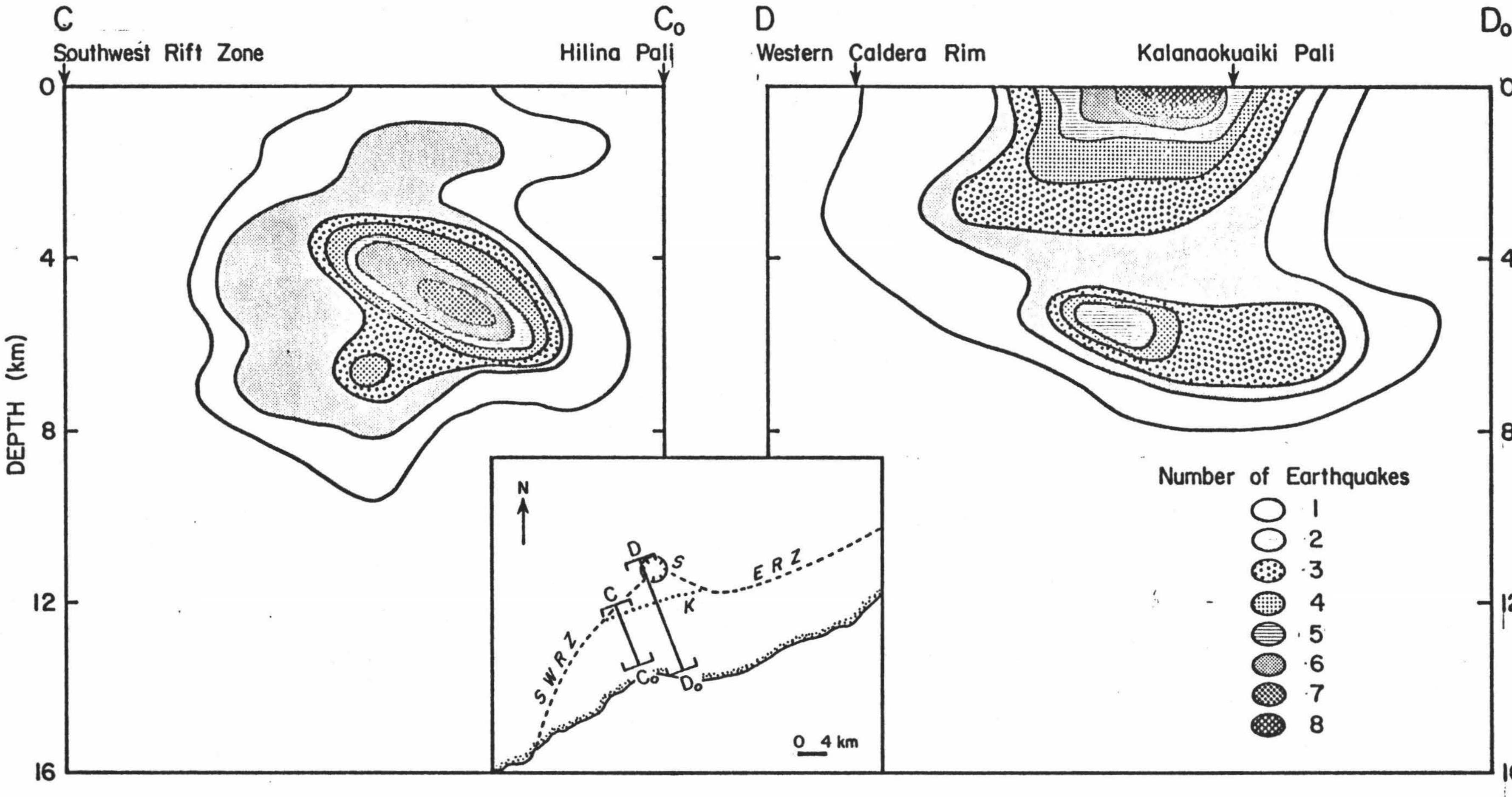
C
Southwest Rift Zone
C_o
Hilina Pali
D
Western Caldera Rim
Kalanaokuaiki Pali
D_o
DEPTH (km)
0
4
8
12
16
N
D
S
E R Z
C
K
S W R Z
C_o
D_o
0 4 km
Number of Earthquakes
1
2
3
4
5
6
7
8

Fig. 11. Composite fault plane solutions for earthquakes located in the Koae fault zone. Solid black quadrants indicate compression, open quadrants indicate dilatation. Other symbols same as Fig. 7.

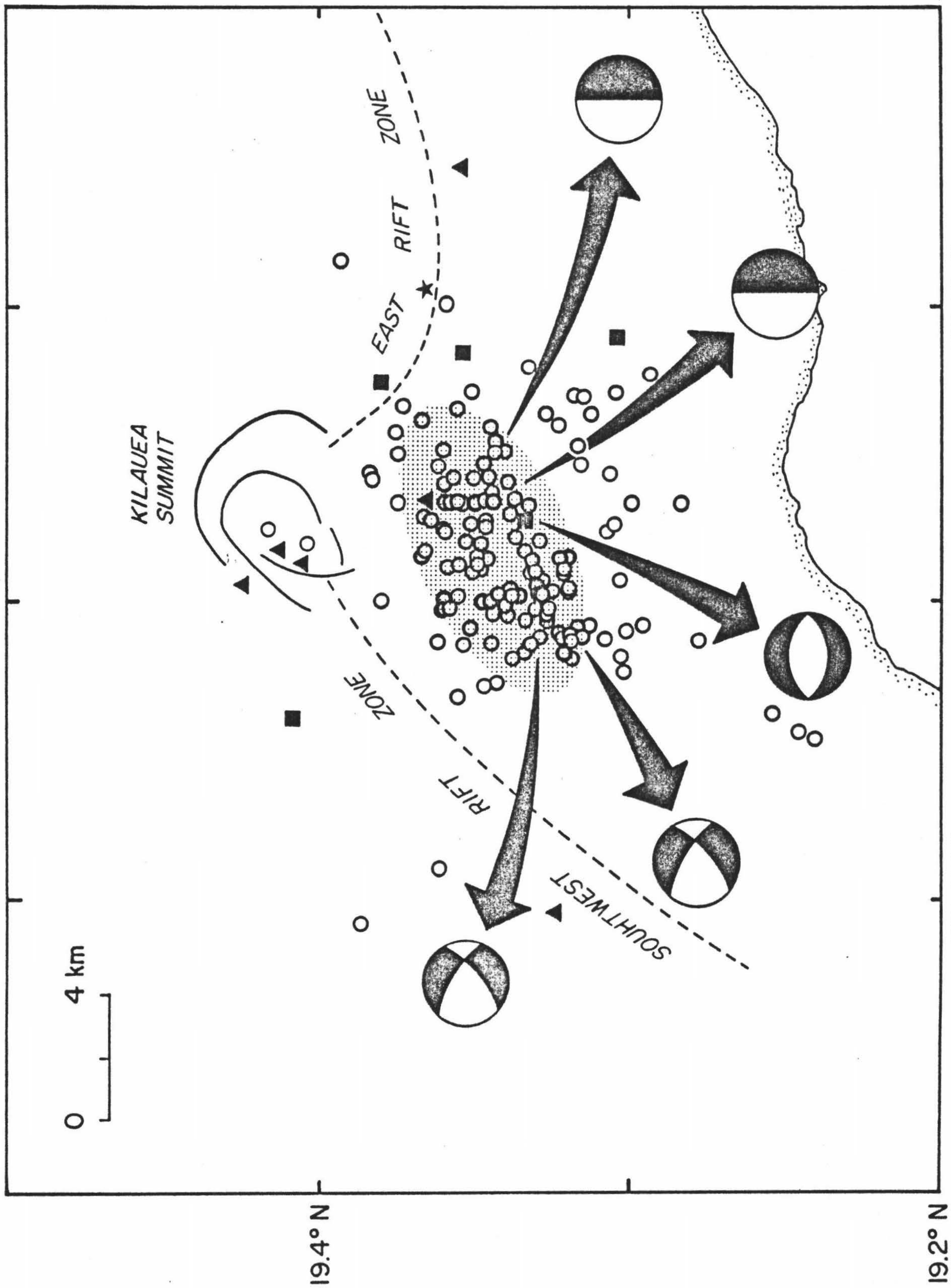
KILAUEA SUMMIT
EAST RIFT ZONE
SOUHTWEST RIFT ZONE
155.2° W
155.4° W
19.4° N
19.2° N
0
4 km

Fig. 12. Fault plane solutions of Fig. 11 plotted in cross section parallel to the Koae. The view of the focal spheres are from the side, looking north, as opposed to Fig. 11 looking down at the lower focal sphere. Open circles are hypocenters.

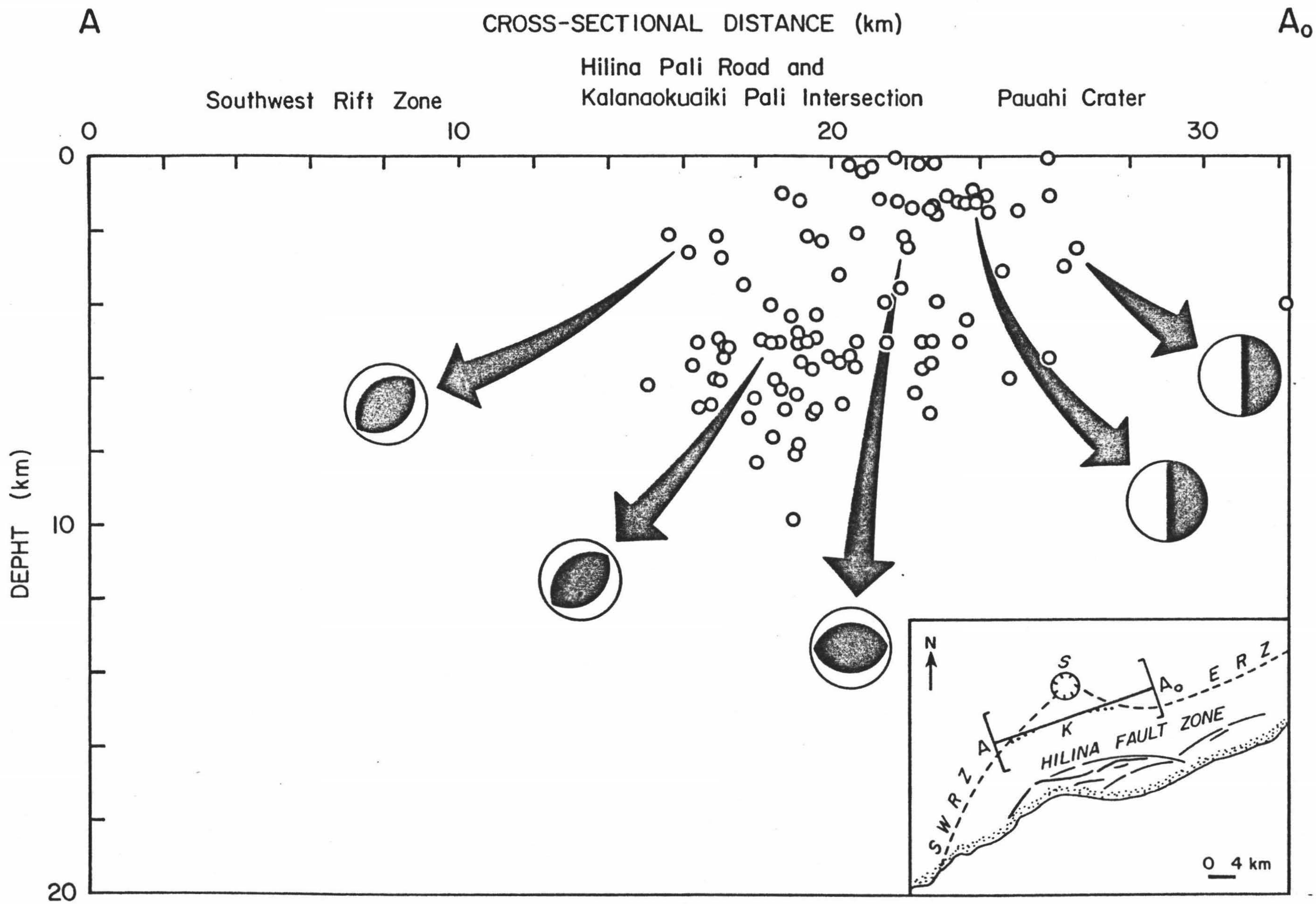

A
CROSS-SECTIONAL DISTANCE (km)
A₀
Hilina Pali Road and
Kalanaokuaiki Pali Intersection
Southwest Rift Zone
Pauahi Crater
0
10
20
30
0
10
20
DEPHT (km)
N
S
K
A
A₀
E R Z
S W R Z
HILINA FAULT ZONE
0 4 km

Fig. 13. Three dimensional view of Kilauea looking to the NE. Stippled plane represents a diffuse shear zone upon which seaward displacement of the south flank of Kilauea may occur. Arrow points in the direction of displacement. Pit craters, cracks, and fault scarps also displayed.

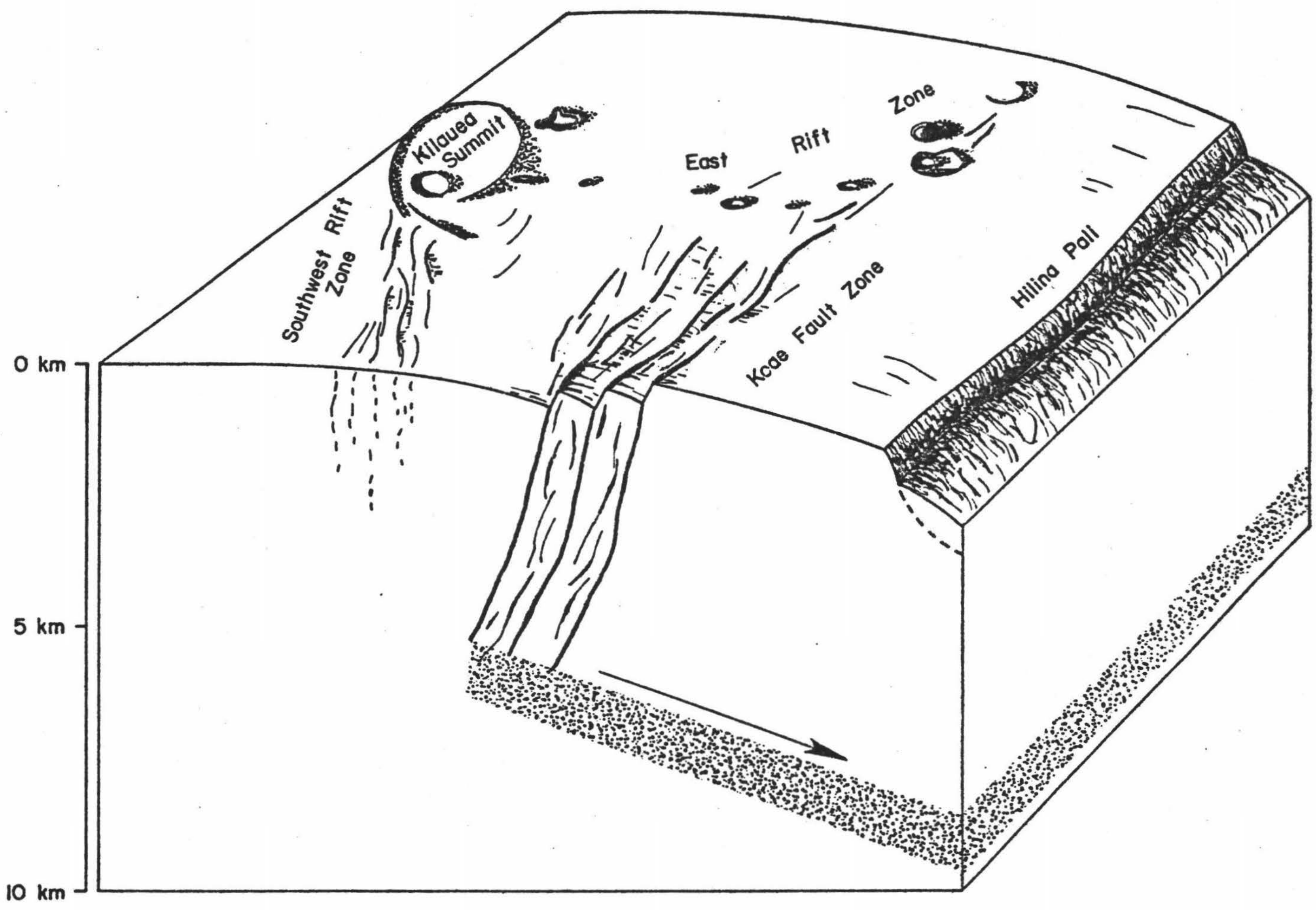
Kilauea Summit
East Rift Zone
Southwest Rift Zone
Koae Fault Zone
Hilina Pali
0 km
5 km
10 km

Fig. 14. Clock drift graph. Station abbreviations listed in appendix B.

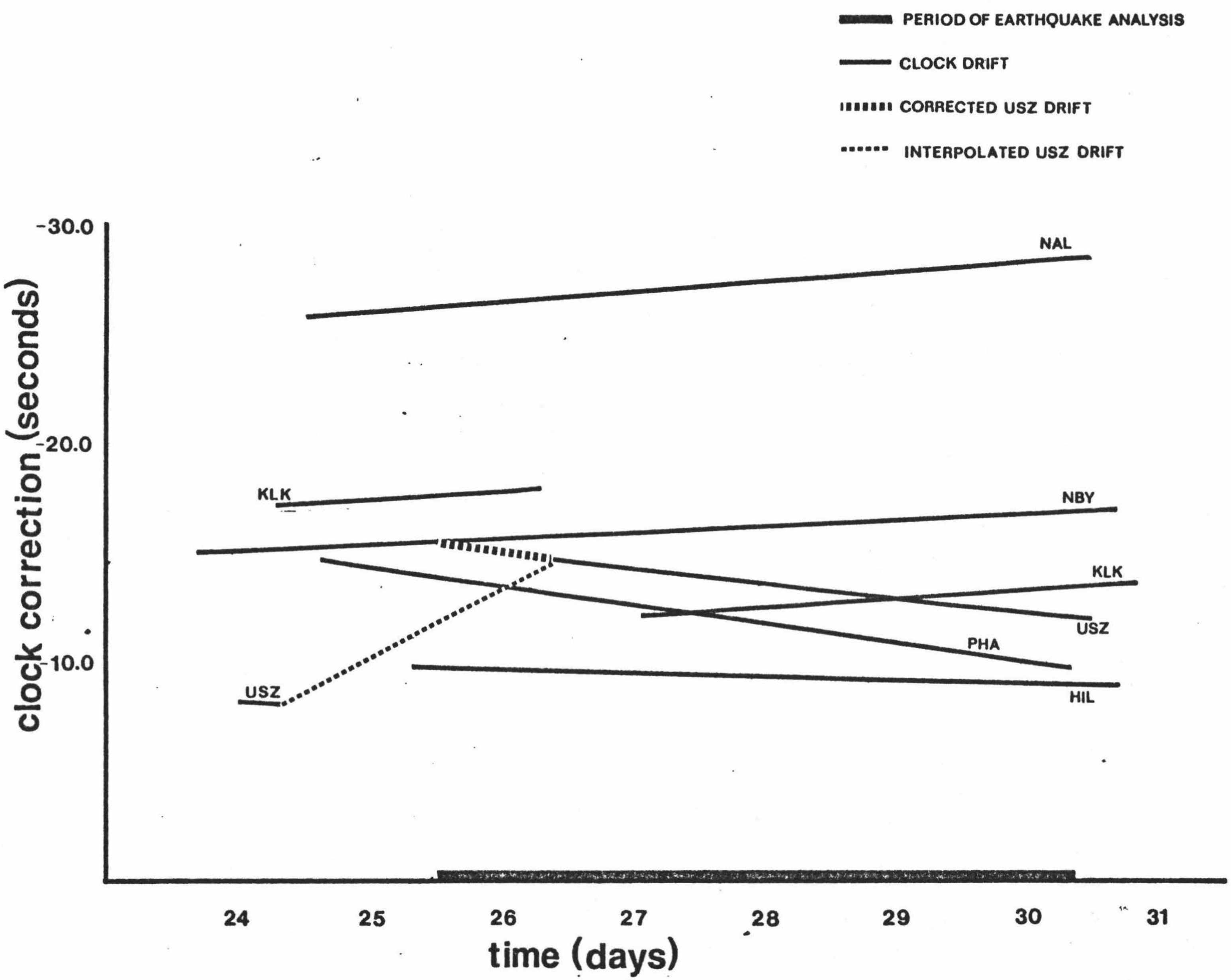
PERIOD OF EARTHQUAKE ANALYSIS
CLOCK DRIFT
CORRECTED USZ DRIFT
INTERPOLATED USZ DRIFT
-30.0
-20.0
-10.0
clock correction (seconds)
NAL
KLK
NBY
KLK
USZ
PHA
USZ
HIL
24
25
26
27
28
29
30
31
time (days)

Fig. 15. Graph of outer station residuals used in determining a correction for the USZ station clock drift.

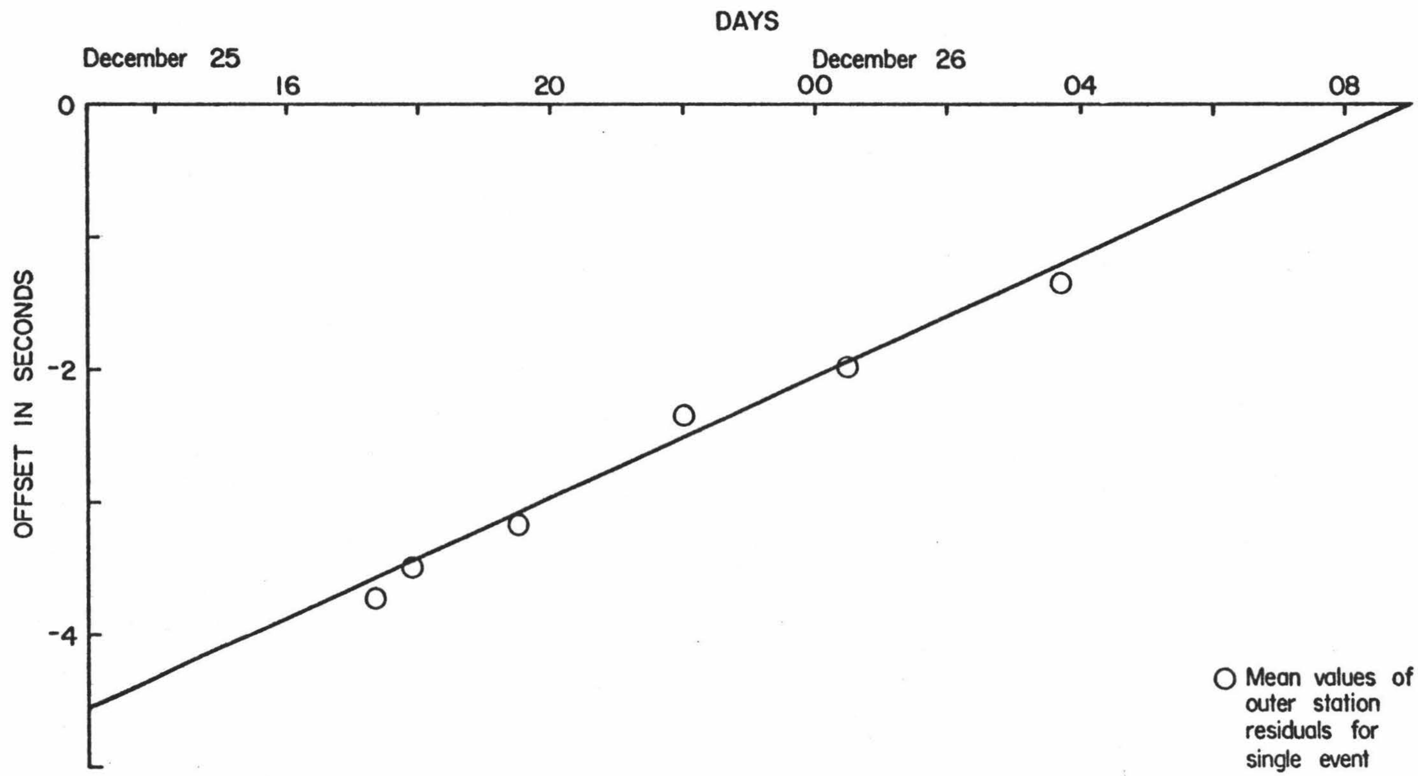

DAYS
December 25
December 26
16
20
00
04
08
0
-2
-4
OFFSET IN SECONDS
Mean values of outer station residuals for single event

REFERENCES CITED

Aki, Keiiti, 1965, Maximum Likelihood Estimate of b in the Formula Log N=a-bM and its Confidence Limits, Bulletin of the Earthquake Research Institute, Tokyo, Vol. 43, 237-239.

Ando, Masataka, 1979, The Hawaii Earthquake of November 29, 1975: Low Dip Angle Faulting Due to Forceful Injection of Magma, Journal of Geophysical Research, Vol. 84, No. B13, 7616-7626.

Asada, T., J. Suzuki, and Y. Tomoda, 1951, Notes on the Energy and Frequency of Earthquakes, Bulletin of the Earthquake Reseach Institute, Tokyo, Vol. 29, 228-293.

Brambaugh, David S., 1979, Classical Focal Mechanism Techniques for Body Waves, Geophysical Surveys, Vol. 3, 297-329.

Carter, Jerry A., and E. Berg, 1981, Relative Stress Variations as Determined by b-Values from Earthquakes in Circum Pacific Subduction Zones, Tectonophysics, in press.

Crosson, R. S., and E. T. Endo, 1981, Focal Mechanisms of Earthquakes Related to the November 29, 1975 Kalapana, Hawaii Earthquake: The Effect of Structure Models, Submitted to Bull. Seismol. Soc. Amer.

Crosson, Robert S., and R. K. Koyanagi, 1979, Seismic Velocity Structure Below the Island of Hawaii from Local Earthquake Data, Journal of Geophysical Research, Vol. 84, No. B5, 2331-2342.

Duffield, Wendell A., 1975, Structure and Origin of the Koae Fault System, Kilauea Volcano, Hawaii, Geological Survey Professional Paper 856, 1-12.

Dzurisin, D., L. A. Anderson, G. P. Eaton, R. Y. Koyanagi, P. W. Lipman, J. P. Lockwood, R. T. Okamura, G. S. Puniwai, M. K. Sako, and

K. M. Yamashita, 1980, Geophysical Observations of Kilauea Volcano, Hawaii, 2. Constraints on the Magma Supply during November 1975-September 1977, Journal of Volcanology and Geothermal Research, Vol. 7, 241-269.

Eaton, J. P., 1962, Crustal Structure and Volcanism in Hawaii, American Geophysical Union Monograph 6, 13-29.

Endo, Elliot T., Jennifer S. Nakata, and R. S. Crosson, 1979, Focal Mechanisms of Crustal and Mantle Earthquakes Beneath the Island of Hawaii, Hawaii Symposium on Intraplate Volcanism and Submarine Geology, Hilo, Hawaii, 160.

Estill, Robert E., Seismotectonics and Velocity Structure of the Southeastern Hawaiian Ridge, 1979, Dissertation, University of Hawaii, 1-110.

Finch, R. H., 1950, The December 1950 Subsidence at Kilauea, The Volcano Letter, No. 510, United States Geological Survey, October-December.

Fiske, R. S., and W. T. Kinoshita, 1969, Inflation of Kilauea Volcano [Prior to Its 1967-1968 Eruption, Science, Vol. 165, 341-349.

Fiske, Richard S., and Robert Y. Koyanagi, 1968, The December 1965 Eruption of Kilauea Volcano, Hawaii, Geological Survey Professional Paper 607, 1-21.

Furumoto, A. S., and R. L. Kovach, 1979, The Kalapana Earthquake of November 29, 1975: An Intra-Plate Earthquake and its Relation of Geothermal Processes, Physics of the Earth and Planetary Interiors, Vol. 18, 197-208.

Hill, David P., Crustal Structure of the Island of Hawaii from Seismic-Refraction Measurements, 1969, Bulletin of the Seismological Society of America, Vol. 59, No. 1, 101-130.

Jackson, Dallas B., and Maurice Sako, 1979, Self-Potential Mapping on the Southwest Rift Zone of Kilauea Volcano, Hawaii, Hawaii Symposium on Intraplate Volcanism and Submarine Geology, Hilo, Hawaii, 165.

Jaggar, T. A., 1938, The Volcano Letter, No. 459 monthly, Department of the Interior, National Park Service, May 1938.

Kinoshita, Willie T., 1968, May 1963 Earthquakes and Deformation in the Koae Fault Zone, Kilauea Volcano, Hawaii, United States Geological Survey Professional Paper 575-C, 173-176.

Klein, Fred W., Pall Einarsson, and Max Wyss, 1977, The Reykjanes Peninsula, Iceland, Earthquake Swarm of September 1972 and Its Tectonic Significance, Journal of Geophysical Research, Vol. 82, No. 5, 865-888.

Koyanagi, Robert Y., Karen Meagher, Fred W. Klein, Gary S. Puniwai, and John P. Lockwood, 1978, Hawaiian Volcano Observatory Summary 77, January to December 1977, 1-76.

Koyanagi, Robert Y., Patricia Stevenson, Elliot T. Endo, Arnold Okamura, J. P. Lockwood, D. W. Peterson, and R. I. Tilling, 1978, Hawaiian Volcano Observatory Summary 74, January to December 1974, with a Chronological Summary, 1-164.

Koyanagi, Robert Y., D. A. Swanson, and E. T. Endo, 1972, Distribution of Earthquakes Related to Mobility of the South Flank of Kilauea Volcano, Hawaii, Geological Survey Research Paper 800-D, 89-97.

Lee, W. H. K., R. E. Bennett, and K. L. Meagher, 1972, A Model of Estimating Magnitude of Local Earthquakes from Signal Duration, United States Geological Survey, Open File Report.

Lee, W. H. K., and L. C. Lahr, 1975, HYPO71 (Revised): A Computer Program for Determining Hypocenter, Magnitude, and First Motion Pattern of Local Earthquakes, United States Geological Survey, Open File Report 75-311, 1-43.

Macdonald, G. A., and A. T. Abbott, 1970, Volcanoes in the Sea, University Press of Hawaii.

Mogi, Kiyoo, 1963, Some Discussions on Aftershocks, Foreshocks, and Earthquake Swarms-the Fracture of a Semi-Infinite Body Caused by an Inner Stress Origin and its Relation to the Earthquake Phenomena, Bulletin of the Earthquake Research Institute, Tokyo, Vol. 41, 615-658.

Moore, James G., and Robert Y. Koyanagi, 1969, The October 1963 Eruption of Kilauea Volcano, Hawaii, United States Geological Survey Professional Paper 614-C, C1-C13.

Richter, Charles F., 1958 Elementary Seismology, W. H. Freeman and Co., 768.

Ryall, Alan and Dale L. Bennett, 1968, Crustal Structure of Southern Hawaii Related to Volcanic Processes in the Upper Mantle, Journal of Geophysical Research, Vol. 73, No. 14, 4561-4582.

Ryan, Michael P., Robert Y. Koyanagi, and Richard S. Fiske, 1981, Modeling the Three-Dimensional Structure of Macroscopic Magma Transport Systems: Application to Kilauea Volcano, Journal of Geophysical Research, in Press.

Scholz, C. H., 1968, The Frequency-Magnitude Relation of Microfracturing in Rock and its Relation to Earthquakes, Bulletin of the Seismological Society of America, Vol. 58, No.1, 399-415.

Shimozuru, D., 1971, A Seismological Approach to the Prediction of Volcanic Eruptions, in: The Surveillance and Prediction of Volcanic Activity, Unesco Earth Science Monograph, Vol. 8, 19-45, Paris.

Swanson, Donald A., 1972, Magma Supply Rate of Kilauea Volcano, 1952-1971, Science, 175, 169-170.

Swanson, Donald A., Wendell A. Duffield, and Richard S. Fiske, 1976, Displacement of the South Flank of Kilauea Volcano: The Result of Forceful Intrusion of Magma into the Rift Zones, Geological Survey Professional Paper 963, 1-39.

Unger, John D., and Robert Y. Koyanagi,1979, Evidence of the effects of Shallow Magma Intrusion on Kilauea Volcano, Hawaii Symposium on Intraplate Volcanism and Submarine Geology, Hilo, Hawaii, 176.

Ward, Peter L. and Soren Gregersen, 1973, Comparison of Earthquake Locations Determined with Data from a Network of Stations and Small Tripartite Arrays on Kilauea Volcano, Hawaii, Bulletin of the Seismological Society of America, Vol. 63, No. 3, 679-711.